

An aerial photograph showing a coastal landscape with dunes and dune valleys. The dunes are covered with sparse, low-lying vegetation, and the valleys are filled with sand. The overall scene is a mix of green and brown tones, indicating a semi-arid or coastal environment.

The impact of aeolian sediment transport on vegetation development in engineered coastal dunes and dune valleys

J.J. Oude Vrielink

The impact of aeolian sediment transport on vegetation development in engineered coastal dunes and dune valleys

Master thesis

to obtain the degree of Master of Science at University of Twente, to be defended on Tuesday May 12, 2020 at 3:00 PM.

By

J.J. Oude Vrielink

Student number: 1478222

Supervising committee

Dr. M.A. Eleveld
Deltares, Unit of Marine and Coastal Systems

Dr. F. Galiforni Silva
University of Twente, Department of Water Engineering and Management

Prof.dr. K.M. Wijnberg
University of Twente, Department of Water Engineering and Management

An electronic version of this thesis is available at <http://essay.utwente.nl>

Cover: aerial photo of cross-shore dune profile in northern part of Spanjaards Duin, showing from bottom to top: beach, engineered foredune, dune valley and old foredune (Gulden, 2018)

Preface

This thesis finalizes my MSc study in Water Engineering & Management at University of Twente. The research has been carried out at the research institute Deltares and was funded by Rijkswaterstaat. The hosting, cooperation and funding is hereby gratefully acknowledged. I would like to thank the entire graduation committee, Marieke Eleveld, Filipe Galiforni Silva and Kathelijne Wijnberg for their interest and feedback during the project. Marieke, thank you for your strong commitment, enthusiasm and for letting me involve in the Spanjaards Duin project team. Bert van der Valk, Gerrit Hendriksen, Stéphanie IJff and Frank van der Meulen, thank you for your practical help and feedback. Special thanks to Bert and Frank for sharing your expertise about dunes and helping me with answering the practical questions in this research. Many thanks to Bart van Westen, Lisa Meijer and Andrea Flores Ramirez for their help and advice in modelling with AeoliS. I would also like to thank my fellow graduate students, Merve and Sophie. Thank you for your mental support, coffee breaks and personal help with QGIS and Python. At last, I would like to thank my family and friends. Due to the corona virus I was forced to spend the last months of my thesis in my home office in Scheveningen. I would like to thank my co-worker and on top of that my girlfriend. Renée, thank you for your mental support and pulling me out of the "thesis bubble" when I needed it.

*J.J. Oude Vrielink
The Hague, April 2020*

Abstract

In 2009 a new dune area was constructed in front of the Delfland Coast. This engineered dune area consists of a foredune and a dune valley and is called Spanjaards Duin. Spanjaards Duin was created as a compensation measure for the expected increase in nitrogen deposition from the expansion of the Rotterdam harbour (Maasvlakte 2). The predefined compensation goal is to reach 6 ha of moist dune slack vegetation and 10 ha of dry grey dune vegetation in 2033. This is pursued by creating favourable abiotic conditions for natural vegetation development (van der Meulen et al., 2014). This research studies three key abiotic influences impacting the development of target habitats. These three influences are: aeolian sediment transport, bed level change and sediment grain size distribution.

Bed level changes and sediment transport pathways were studied in Spanjaards Duin using monitoring data of LiDAR sensors on UAV and airplane. Elevation profiles of the foredune were extracted to study cross-dune morphological development focusing on the influence of planted Marram grass and beach buildings. Bed level changes were analysed in a series of artificial reed bundle fields to identify aeolian sediment transport pathways in the dune valley. A third analysis focused on bed level changes in blowouts located outside Spanjaards Duin as a potential sediment source for the dune valley of Spanjaards Duin. Two types of models were used in this research differentiating in scale. A volume balance approach was used to calculate aeolian sediment transport in Spanjaards Duin on a meso-scale (annual interval). The magnitude of transport was calculated using elevation monitoring data from LiDAR. A simplified direction of transport was assumed using wind measurements. A micro-scale (daily interval) modelling approach was used to model aeolian sediment transport, bed level change and the development of the sediment grain size distribution on the foredune and in the dune valley. For this, the numerical aeolian sediment transport model AeoliS was used (Hoonhout & de Vries, 2016).

Aeolian sediment transport showed to be driven by high magnitude wind events. Aeolian sediment transport pathways on the foredune were directed cross-shore and transport pathways in the dune valley were directed longshore with lower transport rates. This difference in pathway direction was explained by spatial differences in impact of events with Marram grass a key element in reducing aeolian sediment transport. Beach building's influence showed to be minor. AeoliS modelling results showed that bed level change and the sediment grain size are interrelated. In the dune valley aeolian reworking took place which resulted in a non-erodible layer dominated by rough particles. This process resulted in a higher threshold for transport and therefore a stabilized bed level. This process was confirmed by field observations and LiDAR bed level elevation data. In these engineered coastal dunes and dune valleys such as Spanjaards Duin it is concluded that two factors highly influence the abiotic conditions. Marram grass as a bodyguard for reducing aeolian sediment transport and nourished sand by highly influencing the bed level changes and sediment grain size distribution in the dune valley.

Contents

1	Introduction	5
1.1	Spanjaards Duin	5
1.2	Problem statement	7
1.3	Objective and research questions	8
2	Literature review	9
2.1	The beach-dune system	9
2.2	Aeolian sediment transport on a flat bed	11
2.3	Morphology	11
2.4	Vegetation	13
2.5	Fetch	15
2.6	Flow regime	15
3	Methodology	16
3.1	Data analysis	16
3.2	Meso-scale modelling	22
3.3	Micro-scale modelling	23
4	Results	27
4.1	Data analysis	27
4.2	Meso-scale modelling	31
4.3	Micro-scale modelling	32
5	Discussion	36
5.1	Aeolian sediment transport	36
5.2	Bed level change	37
5.3	Sediment size distribution	38
6	Conclusion	39
7	Recommendations	41
A	Maps	43
B	AeoLis model description	48

Chapter 1

Introduction

1.1 Spanjaards Duin

In 2009, a new dune area of 35 ha was created in front of the Delfland Coast located in the south-west of The Netherlands (Figure 1.1). This Dune area called Spanjaards Duin is part of the Natura 2000 area Solleveld-Kapittel-Duinen. Spanjaards Duin was created by a beach and dune nourishment consisting of marine sands from the North Sea. The nourishment resulted in a new foredune constructed in front of the old foredune. In between, a lower dune valley exists. After construction, Marram grass (*Ammophila arenaria*) was planted locally to stabilize the new foredune (van der Meulen et al., 2014). Spanjaards Duin is defined as the area covering the foredune and the dune valley. A map is shown in Figure 1.2.



Figure 1.1: Satellite image (Sentinel-2) of the southwestern Delta of The Netherlands, showing from north to south nature areas (Spanjaards Duin, Van Dixhoorndriehoek, Kwade Hoek, Flauwe Werk and Hompelvoet) and expansion of the Rotterdam harbour (Maasvlakte 1 and 2)



Figure 1.2: Map of Spanjaards Duin

1.1.1 Building (with) Nature

Spanjaards Duin was created as a compensation measure for the expansion of the Rotterdam harbour (Maasvlakte 2). It is expected that activities on the Maasvlakte 2 will cause increased nitrogen deposition (van der Meulen et al., 2014). This increased nitrogen deposition causes damage to Natura 2000 areas located South of the Rotterdam harbour (Figure 1.1). EU regulations oblige that damages or losses to Natura 2000 areas are allowed under strict conditions but always need to be compensated. Spanjaards Duin has been assigned as the location for nature compensation. To fulfill the compensation conditions, vegetation development goals have been set. The predefined goal of the development of Spanjaards Duin is to reach 6 ha of moist dune slack vegetation (H2190) and 10 ha of dry grey dune (H2130) in 2033.

In addition to the vegetation development goal, the offshore construction of Spanjaards Duin aimed to reinforce the Delfland coast. Traditionally, 'hard' protection measures such as groynes were used for the Delfland coast to prevent coastal erosion. From 1990, the policy of reinforcing changed to a more dynamic approach using a soft coastal defense strategy (Hillen & de Ruig, 1993). This approach aims to use the dynamics of the natural system for engineering purposes called Building with Nature (de Vriend et al., 2014). Spanjaards Duin is an excellent example of this since vegetation development stabilizes the dunes and contribute to coastal reinforcement (Jackson & Nordstrom, 2011).

1.1.2 Abiotic conditions

IJff et al. (2017) distinguished three different development phases of natural vegetation development in Spanjaards Duin. It starts with creating favourable abiotic conditions (1) after which vegetation establishment (2) and succession (3) can take place. Abiotic conditions can be explained as the circumstances in and near the soil which are relevant for vegetation establishment. These circumstances are influenced by non biological factors (abiotic) such as precipitation and aeolian sediment transport (caused by wind). It is expected that favourable abiotic conditions related to the soil moisture content and soil chemistry are reached in Spanjaards Duin. However aeolian sediment transport impacts the abiotic conditions too. Aeolian sediment transport impacts the

abiotic conditions directly by determining the amount of sand blasting. High rates of sand blasting can slow down the establishment of target habitats (IJff et al., 2017). Aeolian sediment transport impacts the abiotic conditions indirectly too. This happens firstly by the ability of aeolian sediment transport of changing the bed level. Small accumulation rates stimulate vegetation growth, but high accumulation rates can cause burial of vegetation. Dry grey dune vegetation can cope up with an accumulation rate of 10 cm/year. Erosion of the bed causes vegetation to erode (IJff et al., 2017). Secondly, aeolian sediment transport can change the sediment grain size distribution in the soil. Small sediment particles have higher probability of containing seeds. Favourable sediment grain sizes for moist dune slack vegetation are between 150 and 210 μm . The definitions of these key abiotic conditions including used units in this research are shown in Table 1.1.

Abiotic condition	Definition	Unit
Aeolian sediment transport	The transport rate of sediment volume through the air	$m^3/m/year$ or $m^3/m/day$
Bed level change	The rate of change of the bed level	m/year
Sediment grain size distribution	The grain size distribution of the soil based on fractions of the total mass	-

Table 1.1: Key abiotic conditions related to aeolian sediment transport for moist dune slack and dry grey dune vegetation

1.1.3 Monitoring and management practices

To ensure favourable abiotic conditions are reached and maintained, Spanjaards Duin is monitored and nature management takes place. Vegetation development is heavily monitored for Spanjaards Duin. Vegetation monitoring takes place in positioned permanent quadrants (PQ's). Beside this, possibilities for monitoring of vegetation development with remote sensing are investigated by Deltares. Abiotic factors are also monitored. The groundwater level is an essential factor for natural vegetation development and is therefore measured using ground water level loggers. Data concerning geomorphological development were obtained by collecting bed level measurements using LiDAR. This was performed by Shore Monitoring & Research (Verkerk, 2019) and Rijkswaterstaat (de Graaf et al., 2003). In the past decade Seabuckthorn was manually removed since this species is too dominant and can overgrow target habitat vegetation. Beside this, Marram grass was removed from the valley and replanted on the foredune, and potential blowouts were dug out in the Van Dixhoordriehoek in 2015 (Arens et al., 2016). In January 2019 the dune valley was locally excavated to increase soil moisture content which should enhance the development of moist dune slack vegetation (Arens et al., 2018).

1.2 Problem statement

The increased interest in nature based solutions (Section 1.1.1) results in an increased demand in knowledge of physical processes in the coastal environment. In many Building with Nature projects, vegetation is a key element in the solution and knowledge about the interaction between vegetation and coastal dynamics is required called, biophysical interactions. Existing studies often focus on salt marshes. In these studies the main stresses impacting vegetation development do have a hydrodynamic cause (flooding). A good example is a salt marsh development project on the Wadden Sea coast (The Netherlands) by Baptist et al. (2019). In coastal dunes different stresses such as aeolian sediment transport determine the biophysical interaction. Some studies were done analysing biophysical interactions in dunes but focused on qualitative behaviour (Keijsers et al., 2016) or studied natural formed embryonal dunes (van Puijenbroek et al., 2017), which is not the case for nature based solutions such as Spanjaards Duin. Quantitative knowledge is needed about aeolian sediment transport in man-made coastal dunes and dune valleys.

1.3 Objective and research questions

This research aims to define the quantitative impact of aeolian sediment transport on abiotic conditions for natural vegetation development in engineered coastal dunes and dune valleys. The main research question is stated as follows:

What is the impact of aeolian sediment transport on the abiotic conditions for natural vegetation development in engineered coastal dunes and dune valleys?

To answer the main research question this research puts a focus on the constructed (engineered) foredune and dune valley of Spanjaards Duin. The research is split up in sub-questions. Each sub-question studies a key abiotic condition as presented in Table 1.1. Sub-question 1 studies the aeolian sediment transport itself by focusing on sediment transport pathways in Spanjaards Duin. A sediment transport pathway is defined as the magnitude and direction of annual aeolian sediment transport. Sub-question 2 and 3 focus on the impact on bed level changes and the sediment grain size distribution respectively.

1. *Which aeolian sediment transport pathways exist in Spanjaards Duin?*
2. *What is the impact of aeolian sediment transport on the bed level changes in Spanjaards Duin?*
3. *What is the impact of aeolian sediment transport on the sediment grain size distribution in Spanjaards Duin?*

Chapter 2

Literature review

2.1 The beach-dune system

The beach-dune system can be distinguished in different cross-shore zones (Figure 2.1). Most seaward the surf zone exists in which hydrodynamic processes are responsible for sediment transport. More landward a beach exist on which both hydrodynamic processes and aeolian processes are responsible for sediment transport. Behind the beach the dune area exist where where aeolian processes determine sediment transport rates (Sherman & Bauer, 1993). Focusing on Spanjaards Duin, the dune area consist of (from sea to land) a foredune, dune valley and old foredune.

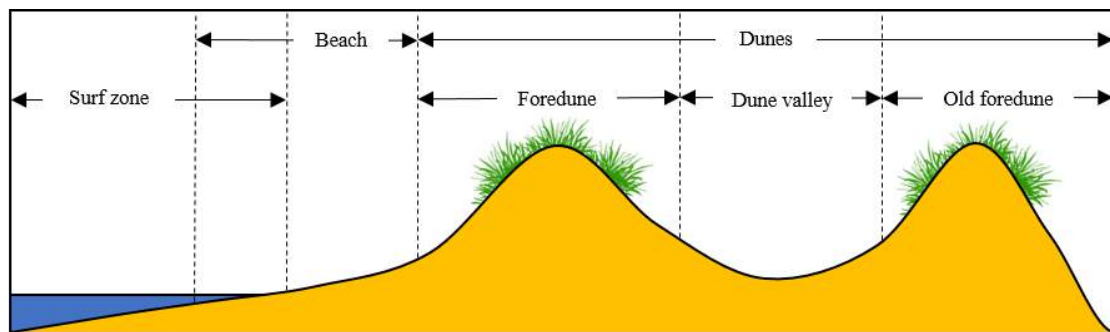


Figure 2.1: Schematization and definition of the beach-dune system based on Sherman and Bauer (1993), and modified to be applicable for Spanjaards Duin

2.1.1 Scales

The beach dune system can be described at three different scale domains in time and space (Sherman & Bauer, 1993). The process scale also defined as the micro-scale describes individual processes. This scale considers hours to months. The second scale is defined as the meso-scale and looks at the behaviour of the whole system and considers periods from months to decades. Looking at a meso-scale the aeolian sediment transport is roughly determined based on two factors: factors influencing the supply of sediment (sediment availability) and factors influencing the transport process itself (transport potential) (Houser & Ellis, 2013). The third scale is defined as the macro scale and considers periods of many decades or longer. This research restricts itself to the first two scales (micro-scale and meso-scale).

2.1.2 Marine processes

In the surf zone hydrodynamic forces are responsible for sediment transport (Sherman & Bauer, 1993). Waves and tides are responsible for marine-driven sediment transport to the lower part of the beach. Sediment transport from beach to the surf zone occurs mostly by storm events which can also cause erosion of the dune (Duarte Campos, 2018). The most simple way of describing the nearshore morphodynamics is using an equilibrium profile approach. This modelling approach defines the beach profile based on the wave height, wave period, beach slope and grain properties.

From this model several conclusions can be drawn with respect to morphodynamic response to forcing: upwards on the beach the profile has a concave shape, steeper beaches occur with larger grain sizes, further offshore profiles become more flat and mild slope profiles are formed with steep waves (Sherman & Bauer, 1993).

2.1.3 Aeolian sediment transport

Three modes of aeolian sediment transport can be distinguished (Bagnold, 1936). Sediment grain size roughly determines the mode of transportation for a sediment particle. Suspension is the mode in which small sediment particles are transported as suspended load in the air. The suspensions mode can be further distinguished in long-term and short-term suspension. Long-term suspension has a suspension time in order of days and transport distance in order of thousands of kilometers. Short-term suspension has a suspension time in order of minutes to hours and a transport distance in order of meters to kilometers. The saltation mode can be explained as the cascade effects when particles collide and overcome the initiation of motion. This mode includes 95% of the total mass transport. Creep is the transport mode which describes particles rolling or pushed along the surface without losing contact with the surface. These particles are too heavy to be lifted by the wind (Nickling & McKenna Neuman, 2009). Diving into aeolian sediment transport requires understanding of different interactions. Best (1993) defined the sedimentary bedform system in terms of feedback between fluid flow, sediment transport and bedform. This review interprets bedform as the bedform including all elements attached to it such as vegetation and substrate properties. A visualization is shown in Figure 2.2. The feedback mechanisms are affected externally by the flow regime. The flow regime can be considered as the forcing of the system and is determined by the magnitude and frequency of flow events (Walker & Nickling, 2002). Factors influencing sediment transport can be divided into two groups: supply limiting factors which influence sediment transport directly by limiting the availability or supply of sediment, and transport limiting factors which influence flow which in turn has impact on the sediment transport.

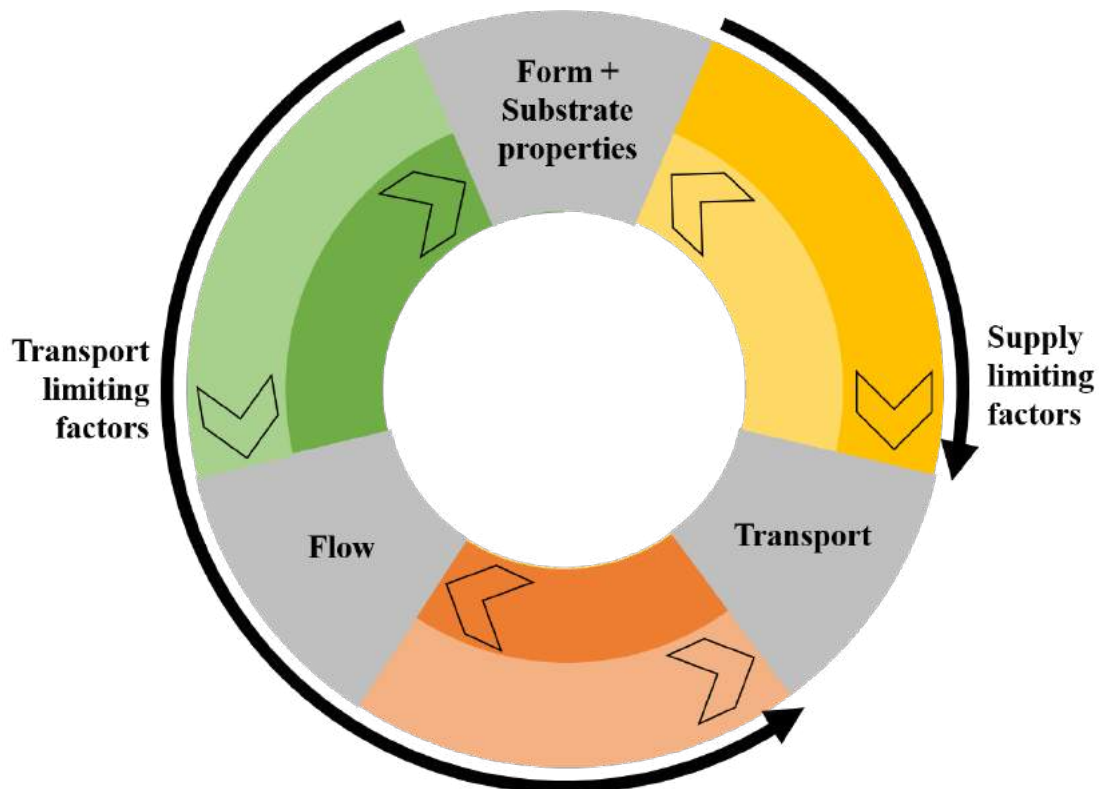


Figure 2.2: Aeolian sediment transport interactions, modified from Best (1993)

2.2 Aeolian sediment transport on a flat bed

Flow over a sandy surface acts a fluid force on sediment particles. When the lift and drag forces of the wind on a particle overcome the weight and cohesion, particles start to move (Houser & Ellis, 2013). An important feedback mechanism is the extraction of momentum from the wind when particles are transported (Walker & Nickling, 2002).

2.2.1 Wind profile

Flow over a flat homogeneous surface is affected by the roughness of the surface layer. This leads to the formation of a boundary layer near the surface, a shear stress acts between the airflow and the surface (Houser & Ellis, 2013). Above the boundary layer the horizontal velocity can be described with a function (Equation 2.1) showing a log-linear increase of horizontal flow velocity with increasing height. This function is known as the Prandtl-von Kármán equation or law of the wall.

$$\frac{u_z}{u_*} = \frac{1}{\kappa} * \ln\left(\frac{z}{z_0}\right) \quad (2.1)$$

Where u_z represents the horizontal air velocity at height z and u_* represents the shear velocity at the bed. κ represents the von Kármán's constant (0.4) and z_0 represents the the areodynamic roughness length which is an indication for the surface roughness (Walker & Nickling, 2002).

2.2.2 Transport modelling

Different models describe the relation between the airflow and aeolian sediment transport. Bagnold (1937) is seen as the first to derive a relation between sediment transport rate and shear velocity, shown in Equation 2.2.

$$Q = C_b * \sqrt{\frac{d}{D}} * \frac{\rho}{g} * u_*^3 \quad (2.2)$$

Where Q represents the saturated or equilibrium transport rate, C_b represents a constant related to the sediment type. d represents the grain size and D a reference grain size. ρ is the air density and g the gravity constant. u_* represents the shear velocity. The threshold shear velocity is calculated using a separate equation constructed using empirical constants, sediment and airflow characteristics (Sherman & Li, 2012). Hoonhout & de Vries (2016) developed an aeolian sediment transport model based on the relation between airflow and the so-called equilibrium aeolian sediment transport rate, shown in Equation 2.2. However, these equilibrium sediment transport rates are often not reached because of limiting factors and spatial variability in sediment transport capacity (Roelvink & Costas, 2019). Therefore AeoliS uses an advection equation to calculate the instantaneous sediment transport rates. A full description of the AeoliS model is shown in Appendix B.

2.3 Morphology

Morphology is a transport limiting factor by its ability to affect airflow and with that the sediment transport (Best, 1993). The surface shear stress over a hill can be explained by two mechanisms called streamline curvature and flow acceleration effects (Walker & Nickling, 2002).

2.3.1 Streamline curvature

Flow over a hill is influenced by the steering abilities of the surface, this is called the streamline curvature effect. Streamline curvature can enhance or dampen the surface shear stress and has therefore influence on the sediment transport (Walker & Nickling, 2002). Two types of streamline curvature can be distinguished. When flow approaches a hill concave streamline curvature occurs at the toe which result in destabilizing effects of the flow. This results in an enhancement of the turbulent flow and an increase in shear stress (Walker & Nickling, 2002) (Figure 2.3 A and Figure 2.4 A and B). At the crest, convex streamline curvature takes place which has the property to stabilize turbulent fluctuations which result lower shear stresses (Walker & Nickling, 2002). Behind

the crest flow separation can take place. According to Bernoulli (1738) an area with lower pressure forms behind the crest under the separated flow stream. The pressure gradient can cause a recirculation of flow backwards to the crest showing an eddy-like structure, which is turbulent flow (Walker & Nickling, 2002) (Figure 2.3 C and Figure 2.4 A). When flow approaches a hill in an oblique angle crest steering of the flow takes place (Bauer et al., 2012). Figure 2.3 B and D show a visualization of this process including expected sediment transport directions.

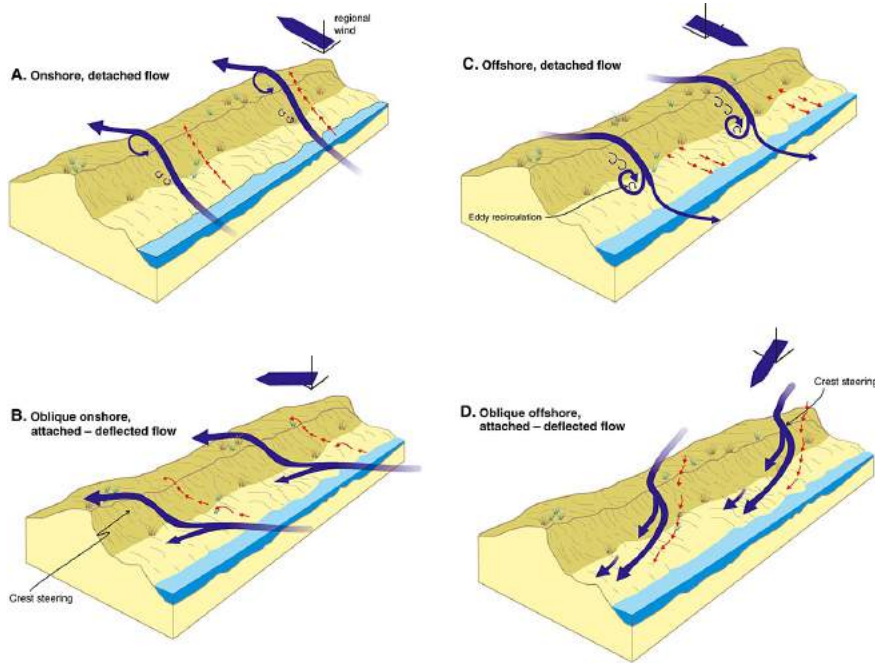


Figure 2.3: Conceptual model of flow-form interaction over large foredunes for variable wind approach directions (A, B, C and D). With in blue the wind flow and red the response of the aeolian sediment transport (Bauer et al., 2012)

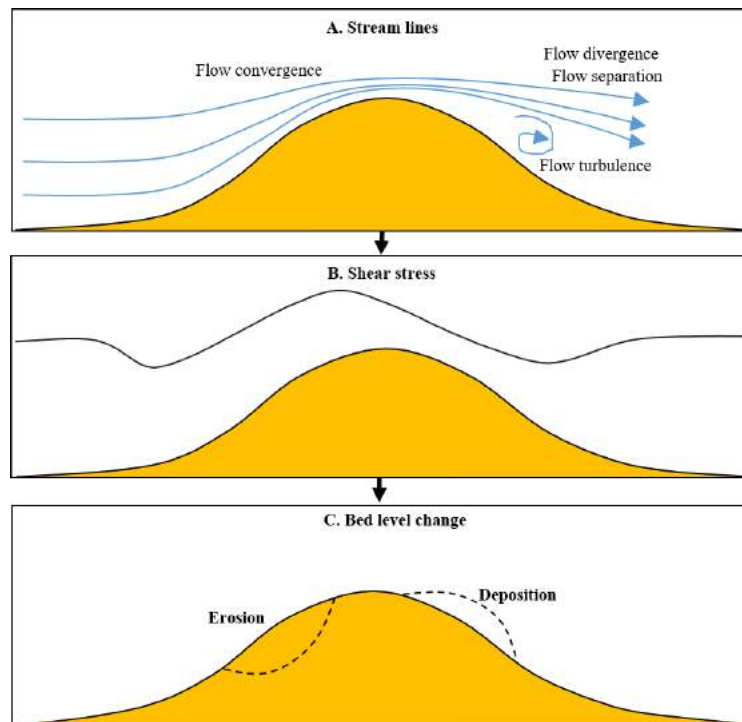


Figure 2.4: Morphological loop showing the relation between flow (A), shear stress (B) and deposition or erosion (C) on an idealized bare dune

2.3.2 Acceleration effects by pressure field

Acceleration effects can be explained by describing the relations between air pressure, wind speed and shear stress near the surface (Figure 2.4 B). A positive air pressure gradient causes a slow down in wind speed (Bernoulli, 1738). Airflow approaching a hill causes a slight increase in surface air pressure in front of the hill caused by stagnation effects. This results in a slight drop in airflow velocity. When moving up the stoss slope of the hill the surface air pressure decreases which results in a speed-up of the airflow velocity. This results in high surface shear stresses and therefore potential for sediment transport. The maximum airflow velocity is reached just before the crest where airflow velocity already starts to decelerate caused by the change in air pressure gradient. On the lee side of the slope the pressure increases which results in a deceleration of the airflow which results in low surface shear stresses (Walker & Nickling, 2002).

2.4 Vegetation

Vegetation can be seen as both a transport limiting factor and a supply limiting factor. Vegetation reduces sediment transport in three ways. Momentum is extracted from the wind by vegetation which increases sediment deposition (transport limiting), vegetation acts as an obstacle by trapping soil particles and area covered with vegetation has no function of sediment supply in the system (supply limiting) (Wolfe & Nickling, 1993). Sediment deposition results in increasing bed levels. The bed level changes in turn influence the growth behaviour of the vegetation. This biophysical interaction can be summarized in a conceptual model shown in figure 2.5 (Zarnetske et al., 2012).

2.4.1 Vegetation as an obstacle

Vegetation affects morphology by its capacity to reduce sediment transport. Arens et al. (2001) studied the influence of vegetation (reed bundles) density on dune profile development. From the results it was shown that higher density vegetation results in slightly higher sediment deposition rates. Furthermore it was concluded that high density vegetation result in steep dune development. Low density vegetation resulted in a more smooth and gradual dune (Arens et al., 2001). The effect of vegetation on sediment transport can be quantified using two different approaches. A first approach looks at the reduction of shear stress near the bed caused by the presence of vegetation (Arens et al., 2001). This reduction in shear stress near the bed can be explained by the change in velocity profile. Wolfe and Nickling (1993) defines two layers of airflow in case of vegetation. The original logarithmic velocity profile is moved upward and located above the vegetation. This layer above the vegetation is called the inertial sub-layer. The layer located inside the canopy is defined as the roughness sub-layer. In this layer turbulent flow exists in the form of wakes behind obstacles. To simplify these processes a second logarithmic profile function is considered to describe horizontal wind flow inside the canopy (Wolfe & Nickling, 1993). To show the effects on sediment transport Raupach (1992) defined an equation for a case with vegetation which relates the friction velocity near the surface U_*s (inside the roughness sub-layer) to the friction velocity just above the vegetation U_*v .

$$\frac{U_*s}{U_*v} = \frac{1}{\sqrt{1 + \beta\lambda}} \quad (2.3)$$

Where β is the ratio between the drag coefficient for roughness elements and bare surface, and λ is the roughness element lateral cover. This approach is often used in process-based models (Cohn et al., 2019; Hoonhout & de Vries, 2016; Roelvink & Costas, 2019). A second approach for quantifying sediment transport with the presence of vegetation is the increase of a threshold shear velocity compared to a situation with a bare surface (Arens et al., 2001).

2.4.2 Biophysical feedback

Vegetation shows dynamic behaviour in the form of growth. The growth behaviour differs amongst species and is held responsible for the rate and shape of dune development (Zarnetske et al., 2012). For this reason it is important to consider growth behaviour. The growth behaviour can be divided in vertical growth and lateral growth.

Vertical growth

The vertical growth speed of vegetation differs per species. An important stress affecting the vertical growth speed of dune species is the burial of vegetation caused by sand deposition. The vertical growth response can be positive in which the sediment deposition stimulates growth, or negative if the vegetation is buried under a layer of sand. The response of the plant depends on the species (Maun, 1998; Zarnetske et al., 2012). Marram Grass needs a moderate to strong sediment accumulation rate of up to 1 m / year (Huiskes, 1979). If the accumulation rate stagnates the vitality of the plant diminishes. Less is known about the burial rates of the target habitats in Spanjaards Duin. In general it can be concluded that dry grey dune vegetation is more vulnerable to burial than Marram grass and that the burial rate should be less than 10 cm / year (Schaminée et al., 1998). The growth response can be modelled as a function of accumulation. Maun (1998) developed a conceptual model considering positive and negative feedback of the growth response, shown in figure 2.5 E. For positive growth responses the function is described with a second-order polynomial. The model applies Shelford's Law of tolerance. This law states that every species performs best around a certain optimum value (Shelford, 1931). This principle is often applied in vegetation response models where vegetation response is highest around a certain sand accretion / burial rate, such as the model of Roelvink and Costas (2019). Keijsers et al. (2016) also defines growth functions based on the sediment accretion, but defines a different growth function for the pioneer stage and established stage of every species. The growth response function of the pioneer stage has optimal growth for high sedimentation rates. Established vegetation has a lower growth rate but can handle higher erosion rates.

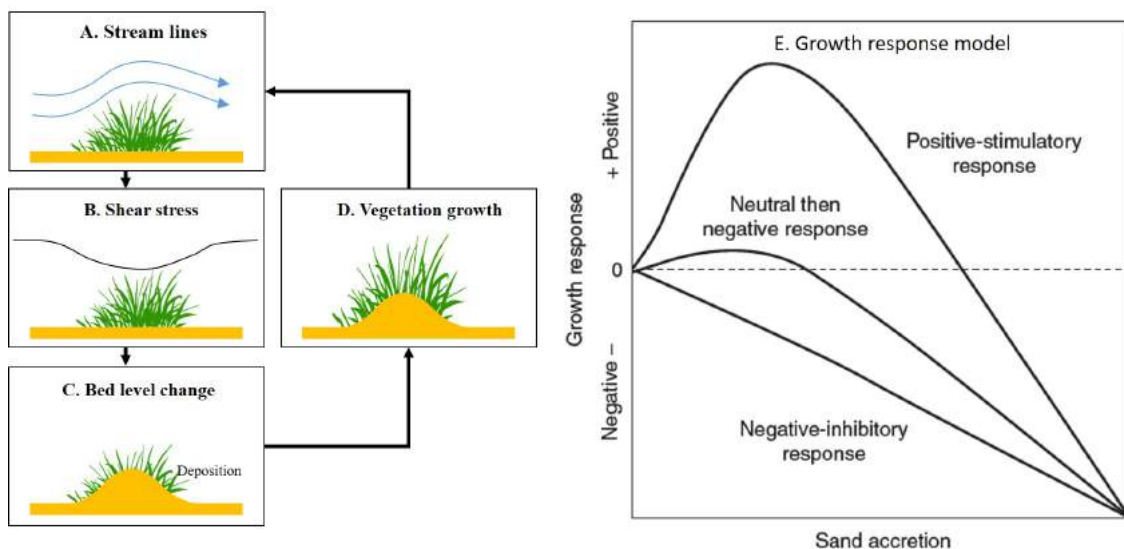


Figure 2.5: Vegetation loop showing biophysical feedback mechanisms (A, B, D and D) and growth response model of Maun (1998) (E)

Lateral growth

Lateral growth happens when vegetation shows a more horizontal growth form. Hacker et al. (2012) studied the difference in growth form between Marram Grass and American beachgrass (*Ammophila breviligulata*) and deposition patterns. The study showed a more vertical growth form with longer vertical rhizomes for Marram Grass resulting in high sediment deposition rates. Meanwhile the American beachgrass showed a more lateral growth form with shorter lateral rhizomes which resulted in lower deposition rates. From Hacker et al. (2012) two growth types can be distinguished. A 'phalanx' expansion type for Marram Grass which uses the resource rich area of close patches, and the 'guerilla' expansion type for American beachgrass which is used by species to escape from resource-poor areas (Ye et al., 2006). Expansion strategy is a second factor which determines lateral growth. When looking at dune species such as *Ammophila arenaria* lateral expansion occurs by spatial shooting. Different expansion strategies can be defined which differ in dispersion over the surface. The most dispersed expansion strategy showed the most potential for sand trapping in terms of total volume. However expansion data for *Ammophila arenaria* showed

an expansion following a Truncated Lévy distribution which corresponds to a more patchy (less dispersed) expansion strategy. It can be concluded that a less dispersed expansion strategy results in less sediment capture but in a higher sand-trapping efficiency because in the latter strategy the rhizomal length is included (Reijers et al., 2019). Modelling lateral expansion is often simplified by defining vegetation coverage which increases when vegetation develops (Cohn et al., 2019; Roelvink & Costas, 2019). The DUBEVEG model of Keijsers et al. (2016) uses a more extensive approach which includes vegetation establishment (lateral expansion) by surrounding vegetation, transport of seeds or rhizome fragments by the wind.

2.5 Fetch

Factors influencing the fetch are considered as supply limiting factors (Figure 2.2). The fetch effect is defined as the increase in sediment transport from a zone with no transport in a downwind direction (Bauer et al., 2009). This zone with no transport can be a saturated foreshore, or the leading edge of a sand sheet. The fetch effect is measured in terms of distance. The principle is that sediment needs to take distance to get suspended in the air, therefore a short fetch distance is associated with low sediment transport rates. The critical fetch distance is the distance at which the maximum sediment transport has been reached (Bauer et al., 2009). Surface moisture influences fetch distance by acting as a limiting transport factor. Surface moisture causes increased cohesion between particles which makes aerodynamic entrainment more difficult. In addition to surface moisture, crusts on the surface act as a supply limiting factor too by functioning as a non-erodible bed surface layer. Crusts can be formed from shells, clay or crystallized salt (Houser & Ellis, 2013). A layer of shells can form after aeolian reworking in which shells stay behind. Especially in nourished environments this process happens which results in lag deposits (Hoonhout & de Vries, 2017; Van der Wal, 2000). Looking at a meso-scale level, the fetch distance is determined by an interplay of the beach width and wind direction. This can be explained by looking at different beachwidths and changing wind directions. A first situation is considered of a narrow beach (smaller than critical fetch length) and a wind from a perpendicular direction with respect to the beach. Transport rates are small caused by the low ability to reach maximum sand transport (short fetch length). Changing to a situation with a wide beach (and a perpendicular wind direction) the sediment transport rates increases, caused by longer fetch length. When changing wind from perpendicular to more oblique a transport increase takes place by increasing fetch distance effect. At the same time a transport reduction occurs, caused by a longer travel distance from beach to dune and less frontal dune area to supply sand. In case of a very oblique angle, the transport reduction dominates the trade-off (Bauer & Davidson-Arnott, 2003).

2.6 Flow regime

The flow regime is considered as the forcing of the aeolian sediment transport system. The flow regime considers frequency and magnitude of wind events. Wind direction is also an important factor and is considered to influence fetch, see Section 2.5. The influence of the flow regime on sediment transport was studied by Delgado-Fernandez and Davidson-Arnott (2011). From this research it was shown that high wind speeds do not generate high rates of sediment transport. This because high wind speeds are often accompanied with limiting factors. These factors include increased moisture contents by waves and short duration of high wind speed events.

Data collection

Since 1970, the Dutch coastal elevation is measured by Rijkswaterstaat. These measurements result in a coastal elevation profile every 5m for the Dutch whole coast, defined as JARKUS profiles. Elevation measurements were taken from an airplane. Between 1970 and 1996 measurements were done with photogrammetry. Since 1996 LiDAR (Light Detection And Ranging) is used. LiDAR measures the distance between the airplane and the surface. Using the flight height of the airplane the surface elevation can be derived. Since the terrain level is of interest and not the surface level, flights were performed between 15 March and 15 April each year at low tide. This period is characterized by a low vegetation cover, therefore errors measuring elevation including vegetation instead of raw terrain elevation were minimized. The points containing vegetation or other objects not representing the terrain were removed by Rijkswaterstaat. The point measurement density varies between 1 and 6 m^2 . For the period 1996-2017 the JARKUS profiles were improved and placed on a grid, this resulted in a DTM map for the Dutch coast (de Graaf et al., 2003). This dataset is further named as JARKUS LiDAR.

As part of the monitoring project of Spanjaards Duin, higher resolution elevation data were collected for the area of Spanjaards Duin (further named as Spanjaards Duin LiDAR) and a smaller sub-area covering the reed bundle fields (further named as Reed bundle LiDAR). These elevation data were collected mainly using LiDAR with an UAV (Unmanned Aerial Vehicle / drone) in the period 2016-2019. It must be noted that the first bed level measurements of the Spanjaards Duin LiDAR dataset (T0) were obtained using a photogrammetry method instead of LiDAR (de Zeeuw, 2016). Nevertheless, for the sake of simplicity all Spanjaards Duin measurements are named as LiDAR measurements. Bed level measurements were collected by the company Shore Monitoring & Research BV. The LiDAR measured the distance between the UAV and the surface. This resulted in a digital surface model (DSM) of Spanjaards Duin. Using a camera also attached to the drone, roughness elements (such as vegetation or houses) in the area could be detected. These points were removed resulting in a DTM consisting of missing data points at roughness element location.

Data structure

The JARKUS LiDAR elevation data were accessed via the repository of Rijkswaterstaat. Data was stored in separated files/maps representing a coastal area. The Delfland coast is stored in map 37an2. The map was stored as a GeoTIFF file. This file contained raster data with a resolution of 5x5m including a georeference embedded in the file.

The Spanjaards Duin LiDAR and Reed bundle LiDAR data were accessed via the repository of Deltares. Data were collected from loose elevation points. The loose elevation points were already filtered for vegetation and placed on a raster resulting in a DTM. A raster with a resolution of 0.5m for the Spanjaards Duin LiDAR was created for: May 2016 (T0), Apr 2017 (T2), Sep 2018 (T4) and May 2019 (T5). For the Reed bundle LiDAR higher resolution measurements were done (0.1m) for: Sep 2016 (T1), Apr 2017 (T2), Sep 2017 (T3), Sep 2018 (T4) and May 2019 (T5). An overview including time coverage was shown in Figure 3.1.

Data quality

Collected raster data of the JARKUS LiDAR were already filtered for outliers, vegetation and objects (de Graaf et al., 2003). No outliers were visible after inspection of the dataset. The uncertainty of a bed level data point was expressed in terms of a standard deviation, and was based on the measurement error and the interpolation error. Measurements errors in the dataset were quantified with validation measurements using GPS. The cause of measurement errors could have several reasons: inaccuracies in laseraltimetry (LiDAR), inaccuracies of GPS validation measurements (height and location) and errors caused by the connection of measurements to the NAP system. Incorporating all different measurement errors it was concluded that the standard error of heights based on measurements was 10 till 15 cm (de Graaf et al., 2003). The dataset contained missing data points which required interpolation. Most of the missing points were observed at location of the buildings near Slag Vlugtenburg, located outside the area of Spanjaards Duin. The amount of missing data differed for each year but ranged between 0.1% and 0.4%. For the calculation of the interpolation error 100 random points were selected. These points were removed and interpolated linearly. A t-test was performed between the 100 points of the original dataset and their interpolated substitution. No significant differences were found between the two

datasets for all measurements in the period 2010-2017. It was concluded that no interpolation error was needed to take into account. Clustering of interpolated points and their variability in space were not taken into account. For the analysis of the accuracy of bed level changes in the JARKUS LiDAR data, a different standard deviation was taken into account. This standard deviation was calculated from the standard deviation of two considered elevations shown in equation 3.1 (Eleveld, 1999).

$$\sigma_{differences} = \sqrt{\sigma_{elevation1}^2 + \sigma_{elevation2}^2} \quad (3.1)$$

In which $\sigma_{elevation1}$ and $\sigma_{elevation2}$ represent the standard errors of separate elevation measurements. This resulted in an error of 0.21 m for bed level changes. Beside the vertical accuracy of bed level measurements, inspection of datasets showed a different spatial alignment between measurements of Mar 2015 and Mar 2016. Therefore bed level changes between Mar 2015 and Mar 2016 were excluded from analysis.

In the Spanjaards Duin LiDAR and Reed bundles LiDAR dataset no outliers were observed. Uncertainties for these higher resolution datasets were assessed in the same way as the JARKUS LiDAR previously described based on the measurement error and the interpolation error. Measurement errors were determined using validation measurements collected with an RTK-GNSS receiver (GPS). Measurements were taken at random ground control points (GCP's) in the field and transects were measured by placing the RTK-GNSS on a wheelbarrow (Gulden, 2018). No outliers were observed in the RTK-GNSS validation measurements. The transect measurements were approached with some skepticism since measurement errors were expected since the wheelbarrow could sink into the sand. Therefore these measurements were not used. Validation measurements for May 2019 (T5) were absent. To determine the measurement error a two sided paired t-test was performed between available GCP validation measurements and the LiDAR measurements at these points. For all datasets the H0 hypothesis could not be rejected which concludes there is no significant difference between RTK-GNSS validation measurements and LiDAR (The H0 hypothesis stated no difference). Gulden (2018) defined a standard deviation for the RTK-GNSS of 0.03m. Therefore this value was assumed as the standard deviation for measurements. Both the Spanjaards Duin LiDAR and the Reed bundles LiDAR contained missing datapoints (Figure 3.2). For the Spanjaards Duin LiDAR data (0.5x0.5m) the percentages ranged between 15% and 18%. The differences in number of missing data points between measurements can be explained by fluctuations in vegetation cover due to the seasons and planting of vegetation in the area. The interpolation error was calculated using the same method as applied for the JARKUS LiDAR dataset. The two sided paired t-test between measured points and interpolated points resulted showed that the H0 hypothesis could not be rejected which concluded no significant interpolation error. Therefore the total uncertainty of an individual elevation measurement for the Spanjaards Duin LiDAR and Reed bundle LiDAR dataset was considered $\sigma=0.03m$. Standard deviations in bed level changes were calculated with Equation 3.1. This resulted in a standard deviation of 0.04 m.

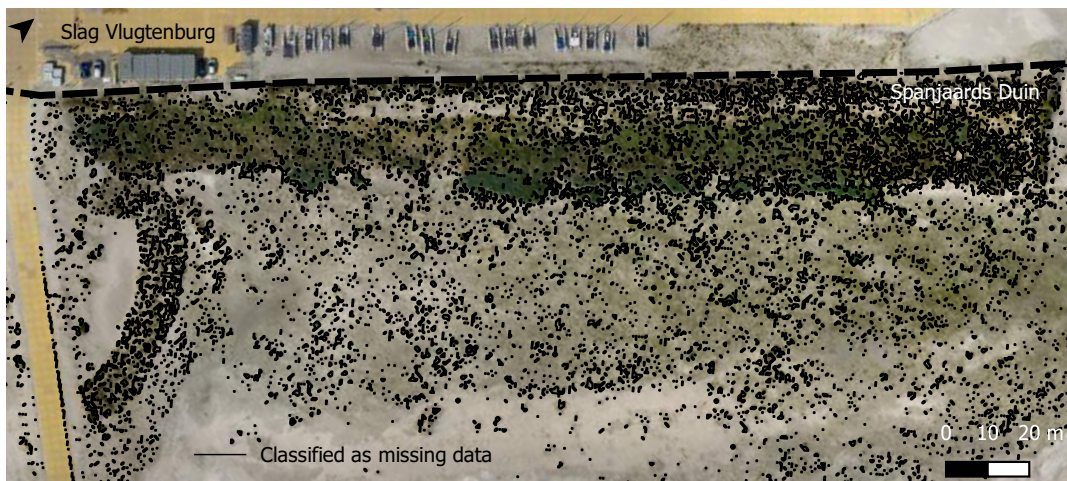


Figure 3.2: Aerial photo of foredune and northern part of the dune valley of Spanjaards Duin, showing contour lines of points which were classified as missing datapoints due to vegetation cover

Data preparation

The JARKUS LiDAR dataset contained all bed level measurements of the Delfland coast. To prepare the JARKUS LiDAR dataset, data was selected on the shape of Spanjaards Duin only (Natura 2000 area with some bandwidth). This shape includes the Van Dixhoordriehoek and a bandwidth of approximately 20 m on the seaside and 100 m on the landside. This bigger shape has been chosen since processes outside the shape of Spanjaards Duin could influence processes inside the area of Spanjaards Duin. Missing datapoints were interpolated using a linear method. In the further interpretation of elevation data an uncertainty of 0.15 m was assumed for bed levels and 0.21 m for bed level changes.

The Spanjaards Duin LiDAR and Reed bundle LiDAR were prepared selecting data for the whole measured area. The measurement area was not constant for different measurements. Therefore elevation differences were only considered for the overlapping part of two measurements. The missing data points were interpolated using a linear interpolation method too. The uncertainty of individual bed level measurements was assumed to be 0.03 m, bed level changes were assumed to have an uncertainty of 0.04 m.

3.1.2 Data analysis

Bed level changes were calculated from bed level elevation data such that a positive bed level change means accumulation and a negative value means erosion of the bed (change = new - old). The bed level changes were converted to a rate in m/year to be able to compare changes between unequal time intervals. After an analysis of the bed level change maps, focus areas were selected for a thorough analysis. A map with an overview of the focus areas is shown in Figure 3.3. The focus areas were selected based on its expected role in determining aeolian sediment transport in Spanjaards Duin. The southern foredune and the blowouts located in the Van Dixhoordriehoek were selected since these areas were situated in and between Spanjaards Duin and possible sediment sources (the beach and the Van Dixhoordriehoek respectively). The reed bundle fields were chosen for its properties to say something about rates and direction of aeolian sediment transport in the dune valley.

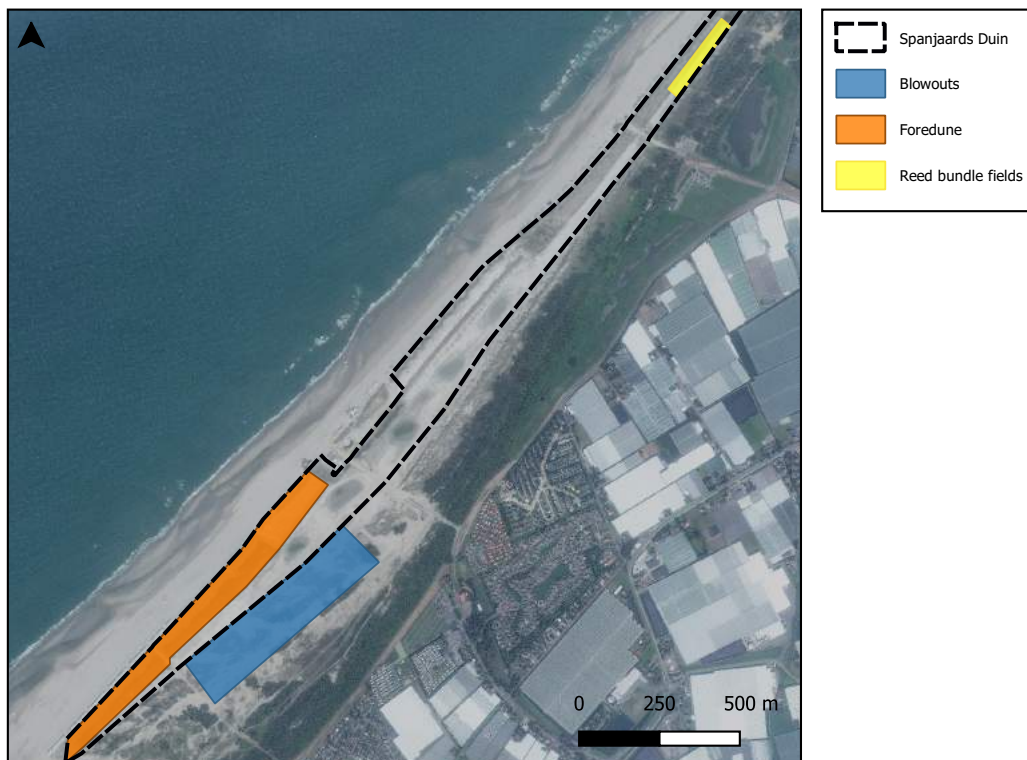


Figure 3.3: Satellite image (SuperView-1) of Spanjaards Duin showing the locations of the focus areas

Foredune

The goal of this analysis was to define how the foredune influenced aeolian sediment transport pathways and bed level changes in Spanjaards Duin. This was done by studying two elements: vegetation and buildings. The studied foredune focusing on vegetation (Figure 3.4: lower constructed foredune) was originally constructed as a bare dune ridge (5.0m+NAP). Behind the foredune, the southern dune valley of Spanjaards Duin is located. In 2013 the foredune was planted with Marram grass on the stoss and lee side to prevent further sedimentation in the valley (Arens et al., 2013). In March 2018 extra Marram grass was planted such that the whole foredune was covered with vegetation (Arens et al., 2018). The foredune parts focusing on the influence of beach buildings were constructed at 7.5m+NAP. In front of the most south located area (Figure 3.4) beach houses are positioned outside the Natura 2000 area on the beach with a distance of approximately 6 m from the toe of the foredune. The beach houses are situated in the area from March till October. Beach houses are positioned along the beach in rows of approximately 20 houses with a distance of 15 m between the groups. To be able to study the influence of beach houses a second area without beach houses was selected as a reference (Figure 3.4: foredune without beach houses). After inspection of aerial photos both areas were assumed to have an equal vegetation cover. Expecting the beach as the main sediment source for this area, it was expected that aeolian sediment transport would mostly take place from beach into the foredune. The planting of Marram grass in 2013 on the lower constructed foredune was expected to capture sediment and therefore would result in morphological dune development. The beach houses located in the South of Spanjaards Duin were expected to function as a sand barrier which could limit morphological dune development. To study morphological dune development elevation difference maps and cross-dune elevation profiles were created from the JARKUS LiDAR data covering the period Mar 2010 till Mar 2017, and the Spanjaards Duin LiDAR covering the period May 2016 (T0) till May 2019 (T5). The influence of the planting of vegetation strips on the morphological development was studied by a comparison between cross-dune profiles before and after 2013. The impact of beach houses on aeolian sediment transport patterns was studied by a comparison of bed level changes between the foredune with and without beach houses.



Figure 3.4: Aerial photo (Gulden, 2018) of southern foredune of Spanjaards Duin, showing selected areas for analysis. Aerial photo taken in Sep 2018

Reed bundles

Bed level changes inside the reed bundle fields were studied using the Reed bundle LiDAR data. The reed bundle fields are located in the most northern part of Spanjaards Duin. Reed bundles were placed in the valley to reduce sediment fluxes near the bed and to create small rates of accumulation to enhance the development of dry grey dune vegetation. In the original situation aeolian sediment transport rates were too high for natural establishment of dry grey dune vegetation (Eleveld & van der Valk, 2019). The experiment consists of four reed bundle fields with each field divided in four strips of different reed bundle density. The set-up of the experiment is shown in Figure 3.5 and Table 3.1. The fields were constructed with a distance of approximately 30 m from each other. The experiment started with field A only, and extended with an extra field after monitoring. The order of expansion was from North to South (A, B, C, D) (Eleveld & van der Valk, 2019). This resulted in 3 elevation measurements for field D, 4 elevation measurements for field C and 5 elevation measurements for field A and B.

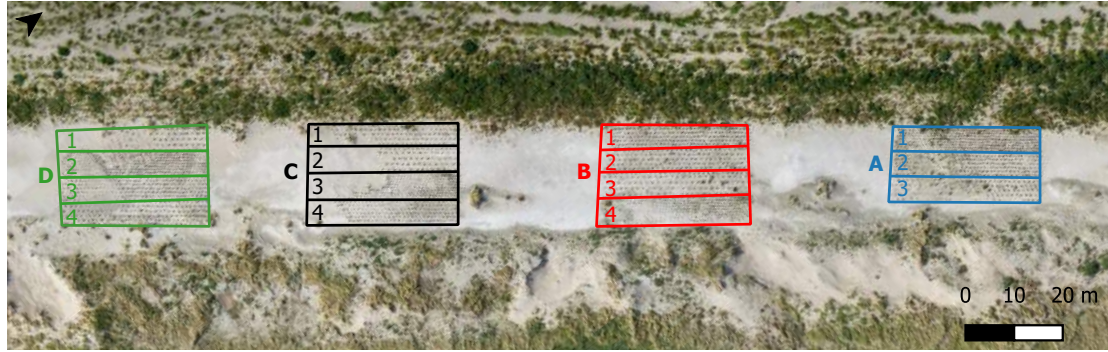


Figure 3.5: Aerial photo (Gulden, 2018) of most northern part of valley, showing the set-up of the reed bundle experiment. Fields are indicated as A, B, C and D, strips are indicated with numbers 1, 2, 3 and 4. Aerial photo taken in Sep 2018

	A	B	C	D
1	2.8 bundles / m^2	1.6 bundles / m^2	1.0 bundles / m^2	0.7 bundles / m^2
2	1.6 bundles / m^2	1.0 bundles / m^2	0.7 bundles / m^2	2.8 bundles / m^2
3	1.0 bundles / m^2	0.7 bundles / m^2	2.8 bundles / m^2	1.6 bundles / m^2
4	-	2.8 bundles / m^2	1.6 bundles / m^2	1.0 bundles / m^2

Table 3.1: Density of reed bundles for different fields (A, B, C and D) and strips (1, 2, 3 and 4)

Sediment was expected to be deposited in all the reed bundle fields. Deposition patterns of all fields were expected to reveal sediment transport direction in this part of the dune valley. In case of a cross-shore sediment transport direction, fields would show same deposition patterns. In case of a sediment transport direction through the valley, fields were expected to influence each other. E.g. a reed bundle field sheltered behind another is expected to show lower deposition rates since the sediment supply is lower. Furthermore, focusing on deposition patterns within a field, it was expected to see higher deposition rates in a strip with higher reed bundle density (Table 3.1). This since high vegetation density leads to higher sediment deposition rates (Arens et al., 2001). Accumulation rate maps were created from the Reed bundles LiDAR data. Due to the unequal intervals between measurements (Figure 3.1), elevation differences were converted to accumulation rates in m/year. This was done to allow for a proper comparison between intervals. Total volume changes of fields were analysed using a boxplot analysis.

Van Dixhoorndriehoek

The aim of this experiment was to study the influence of the Van Dixhoorndriehoek area on aeolian sediment transport pathways in Spanjaards Duin. The Van Dixhoorndriehoek is located south-east of Spanjaards Duin (Figure 1.2). Management practices took place in 2015 in which vegetation was removed from the area and existing blowouts were dug out to stimulate further development (Arens et al., 2016). The management practices performed in 2015 to increase the dynamics were expected to result in a (temporary) sediment source possibly influencing aeolian sediment transport in Spanjaards Duin. The analysis focused on the morphological development of single blowouts located adjacent to the southern Spanjaards Duin valley (from North to South: A, B, C and D, see Figure 3.6). It was assumed that high erosion rates would happen when the blowout was highly exposed to wind (high flow convergence, see Figure 2.4 A). Accumulation rate maps were created based on Spanjaards Duin LiDAR data. These elevation difference maps were compared with KNMI wind climate data collected in Hoek van Holland. It was tried to link wind direction to erosion patterns in blowouts.

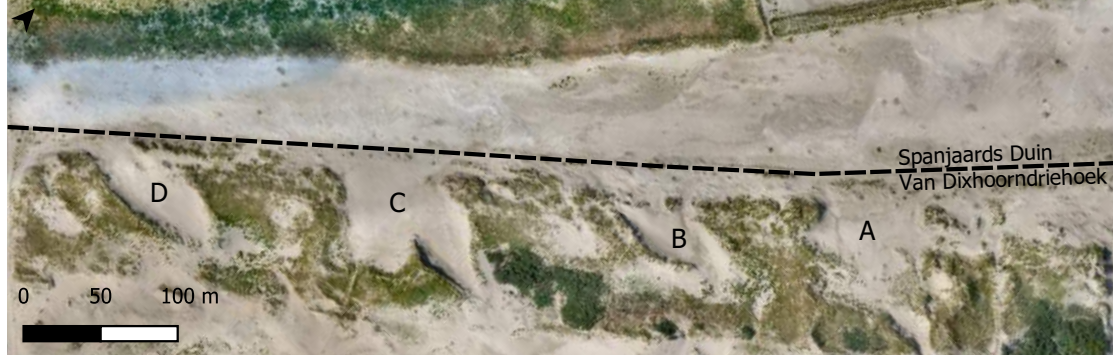


Figure 3.6: Aerial photo of southern valley of Spanjaards Duin (Gulden, 2018), including definition of blowouts

3.2 Meso-scale modelling

A meso-scale modelling approach was used to study aeolian sediment transport pathways in Spanjaards Duin focusing on an annual scale. Aeolian sediment transport could not be observed directly from data since only bed level measurements were measured. However, the aeolian sediment transport pathways could be modelled by deriving the transport direction from the wind climate and the volumetric transport rate from bed level changes.

3.2.1 Meso-scale aeolian sediment transport model

The meso-scale aeolian sediment transport model was defined on a spatial grid. The output of the model is the annual aeolian sediment transport rate in $m^3/m/year$ on every grid cell. This aeolian sediment transport rate was calculated using a volume balance for every grid cell in which sediment volume (V) can enter and leave horizontally (x and y-direction) or vertically (z-direction), see Equation 3.2.

$$V_{in} = V_{in,x} + V_{in,y} + V_{in,z} \quad (3.2)$$

Vertical bed level changes (Δz in m/year) determine how much volume enters or leaves a grid cell (cellsize in m) in vertical direction, this is shown in Figure 3.7 A and Equation 3.3. The -1 accounts for the inverse relation between the bed level change and volume entering a grid cell in z-direction.

$$V_{in,z} = -1 * \Delta z * cellsize^2 \quad (3.3)$$

The amount of volume entering a grid cell in horizontal direction ($V_{in,x}$ and $V_{in,y}$) is fully dependent on the volume leaving adjacent upwind cells. This is shown in Figure 3.7 B. Assuming the volume balance, the total volume leaving a cell should be equal to the total volume entering a cell, shown in Equation 3.4.

$$V_{out} = V_{in} \quad (3.4)$$

The partitioning of the total volume leaving a cell in x and y-direction was calculated using the wind climate. This was done using a vector approach. A single wind event can be expressed as wind speed in x and y-direction, since wind speed events contain a magnitude and direction. All vectors of single wind speed events were summed in which the wind speed was taken to the power three. This was done to include the relation between wind speed and the aeolian sediment transport rate shown in equation 2.2 (Bagnold, 1937). The direction (θ) of this total vector was assumed to be the direction of aeolian sediment transport. The equations for partitioning between x and y-direction are shown in Equation 3.5 and 3.6 respectively.

$$V_{out,x} = V_{out} * \sin(\theta)^2 \quad (3.5)$$

$$V_{out,y} = V_{out} * \cos(\theta)^2 \quad (3.6)$$

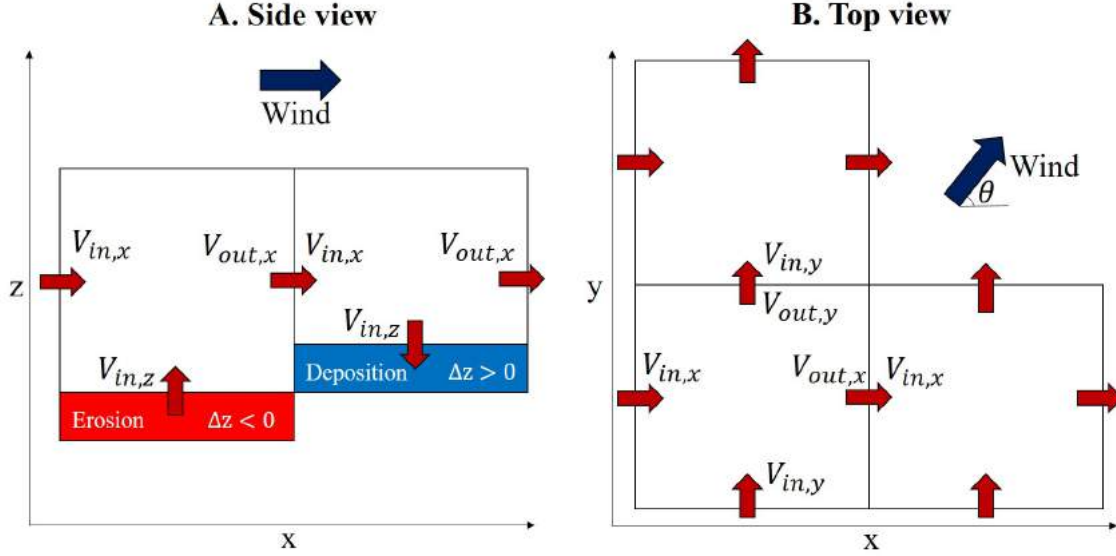


Figure 3.7: Visual explanation of the volume balance of the grid cells used in the meso-scale aeolian sediment transport model showing side view (A) and top view (B). Sediment transport volumes are indicated with red arrows and wind direction is indicated with a blue arrow

3.2.2 Model set-up

For the bed level changes the JARKUS LiDAR data was used. This dataset was chosen for its properties to contain a constant interval between measurements and covering the whole period of the year (Figure 3.1). The sediment transport direction needed for determining the distribution of sediment leaving a grid cell in x and y-direction was calculated from the wind climate data of KNMI (2020). On the boundaries of the schematization, aeolian sediment transport rates from the numerical aeolian sediment transport model AeoliS (Hoonhout & de Vries, 2016) were assumed.

3.3 Micro-scale modelling

A micro-scale modelling approach was used to simulate aeolian sediment transport on the foredune. This approach was used to study the behaviour of the sediment size distribution, bed level change and aeolian sediment transport on a detailed level. Using the modelling results, research sub-questions 1, 2 and 3 were answered.

3.3.1 AeoliS

For the simulation the numerical aeolian sediment transport model AeoliS was used (Hoonhout & de Vries, 2016). AeoliS is a 2DH model which calculates multi fractional aeolian sediment transport for each sediment fraction individually. Aeolian sediment transport is calculated with a traditional aeolian sediment transport model (Bagnold, 1937) and an advection equation (Hoonhout & de Vries, 2016). AeoliS defines three different types of vertical layers (Figure 3.8). The top layer on the surface is called the bed surface layer, the layers below are defined as bed composition layers. Below the bed composition layer a base layer is situated which contains an unlimited amount of sediment. The bed surface layer is the only layer which interacts with the wind, therefore sediment only leaves a grid cell via the bed surface layer. When sediment is picked-up from a grid cell sediment is replaced from the bed composition layer below. Vice versa when sediment is deposited, sediment is excessed to the bed composition layer below. A visualization of this is shown in Figure 3.8. This approach exchanging sediment between layers can be seen as incorporating the vertical dynamics of the bed surface layer. Beside this, an important feature of AeoliS is the incorporation of vegetation. The shear stress reduction caused by vegetation (section is calculated using the vegetation cover (ρ_{veg}) and is based on Raupach et al. (1993). Vegetation growth is based on DUBEVEG (Keijsers et al., 2016) and is specified in AeoliS using a vegetation growth rate

(V_{veg}) and a constant which incorporates the influence of burial (γ_{veg}). A full model description is shown in Appendix B.

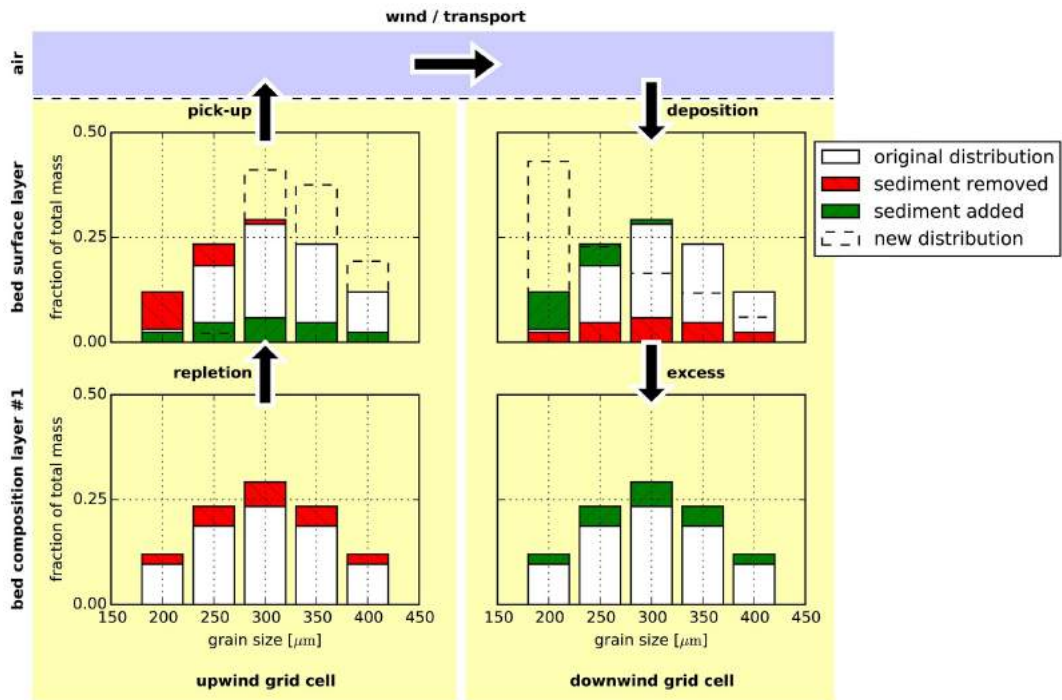


Figure 3.8: Schematization of bed composition discretization in AeoliS, in which the new distribution after transport is shown which indicates that the upwind grid cell becomes coarser and the downwind grid cell becomes finer due to non-uniform erosion and deposition (Hoonhout & de Vries, 2016)

3.3.2 Model set-up

The lower constructed foredune was selected to implement in the model to allow for model validation using observed elevation data (Figure 3.9). The elevation measurements from March 2014 were selected as a starting point for the model schematization. This starting point was selected since significant morphological development was observed after March 2014, caused by the planting of two vegetation strips on the foredune in 2013. The beach was schematized as a linear profile with a width of 75 m.

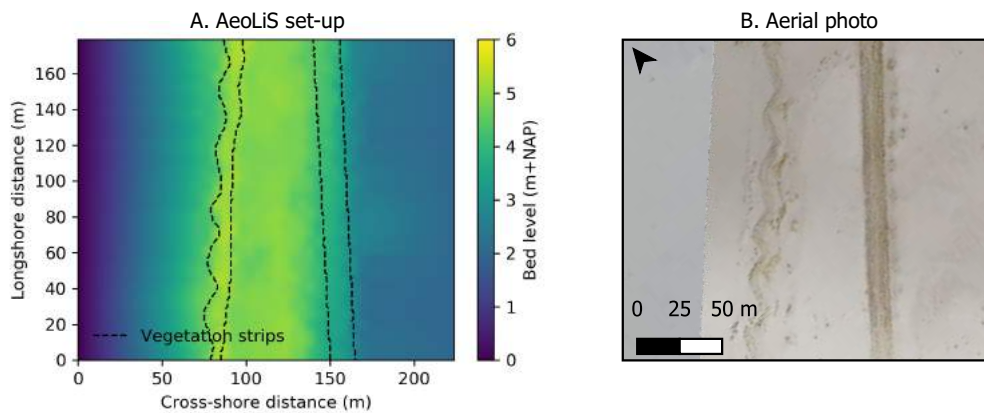


Figure 3.9: Initial model set-up of AeoliS (A) and aerial photo (B) taken in Apr 2017 (de Weger, 2017) showing the bed level elevation and location of vegetation strips on the lower constructed foredune. North Sea on the left side of the figure

The ground water table was implemented in AeoliS by specifying a non-erodible layer. During monitoring period, measurements of the ground water table were done at several locations in Spanjaards Duin. Continuous measurements done in 2016 were analysed for the foredune. It was seen that the groundwater table was far below the surface level. Therefore no non-erodible layer was defined under the foredune. At location of the beach a non-erodible layer was defined at 5cm under the initial bed level. This was done to prevent simulating non desirable erosion rates on the beach (outside the study area), resulting in a constant bed level of the beach. This resulted in hydrodynamic sand supply as the only sediment source for the foredune. Simulations were done for a multi sediment fraction soil composition. A simplified measured sediment grain size distribution was used from measurements done in August 2017 (Figure 3.10). Measured results were reduced to 5 fractions for the model. One extra sediment fraction was added to represent the shells existent in the soil. For this largest grain size the d_{n50} was taken, calculated from the average weight of 30 shells from the dune valley of Spanjaards Duin (collected on 12-03-2020).

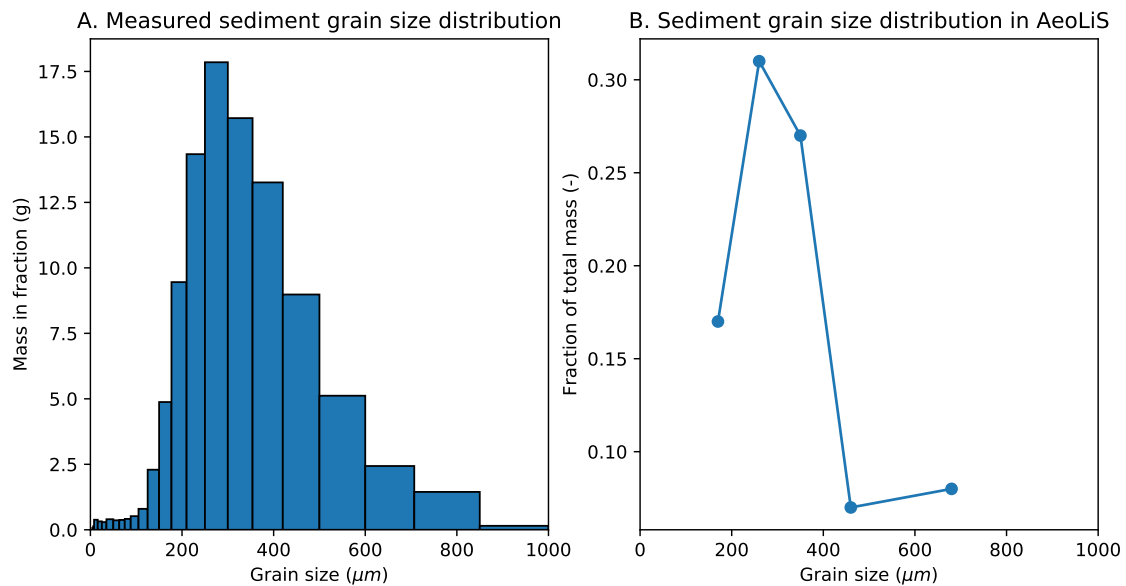


Figure 3.10: Measured sediment size distribution of the southern valley of Spanjaards Duin in August 2017 (Arens et al., 2018) (A) and sediment size distribution modified for AeoliS (B)

The area assigned to the vegetation strips was determined manually using aerial photos of the lower constructed foredune. A constant vegetation density was assumed inside the vegetation strips. Vegetation lateral expansion and growth were not included in the model. However vegetation was assumed to cope up with the bed level changes. Inundated grid cells are reset to initial bed level. For this reason the hydrodynamic processes are responsible for the sediment supply (explanation in Appendix B). The water level was calculated based on tidal elevation from Hoek van Holland and wave run-up in terms of significant wave heights from the Eurogeul (Rijkswaterstaat, 2020). Wind forcing was implemented using the wind climate from Hoek van Holland (KNMI, 2020). All model parameters are shown in Table 3.2. The model was calibrated by adjusting the vegetation density and comparing the simulated bed level profile after 1 year of simulation with the monitored bed level after one year. To study the role of the vegetation strips different simulations were performed. The set-up was changed by removing all vegetation strips and removing one vegetation strip from the simulation (Table 3.3).

Model parameters			
$n_{fraction}$	Number of sediment fractions	6	-
n_{layers}	Number of layers	3	-
d_{layer}	Layer thickness	0.05	m
$d_{sediment}$	Sediment sizes	0.17, 0.26, 0.35, 0.46, 0.68, 6	mm
$dist_{sediment}$	Sediment grain size distribution	0.17, 0.31, 0.27, 0.08, 0.1	-
ρ_{air}	Air density	1.225	kg/m^3
$\rho_{sediment}$	Sediment density	2650	kg/m^3
T_{dry}	Adaptation time scale for soil drying	7200	s
T	Adaptation time scale for advection equation	1.0	s
β	Ratio between drag coefficient of roughness elements and bare surface	130	-
bi	Bed interaction factor	0	-
$accfac$	Numerical acceleration factor	1	-
V_{veg}	Characteristic vegetation growth	0	m/s
γ_{veg}	Constant on influence of sediment burial	0	-
ρ_{veg}	Vegetation cover	0.1	-

Table 3.2: General model parameters used in AeoliS

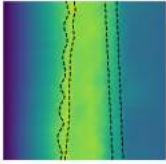
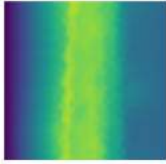
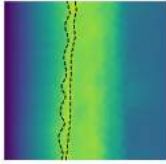
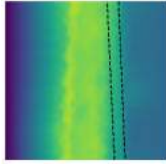
Simulation Parameters		Simulation 1	Simulation 2	Simulation 3	Simulation 4	
nx	Cells in x-direction	224	224	224	224	-
ny	Cells in y-direction	179	179	179	179	-
Δx	Cell size in x-direction	1	1	1	1	m
Δy	Cell size in y-direction	1	1	1	1	m
Δt	Time step	1800	1800	1800	1800	s
t_{stop}	Simulation length	31536000 (1 year)	31536000 (1 year)	31536000 (1 year)	31536000 (1 year)	s
Vegetation set-up		Real situation	Without vegetation	Vegetation on shore side only	Vegetation on valley side only	-
						

Table 3.3: Simulation parameters used in AeoliS

Chapter 4

Results

4.1 Data analysis

4.1.1 Foredune

The foredune of Spanjaards Duin shows in general positive bed level changes, but rates differ per area (Figure 4.1). Beside this, erosion is observed between the lower constructed foredune and the foredune without beach houses which indicates an aeolian sediment transport pathway from the beach into the dune valley (Figure 4.1 B).

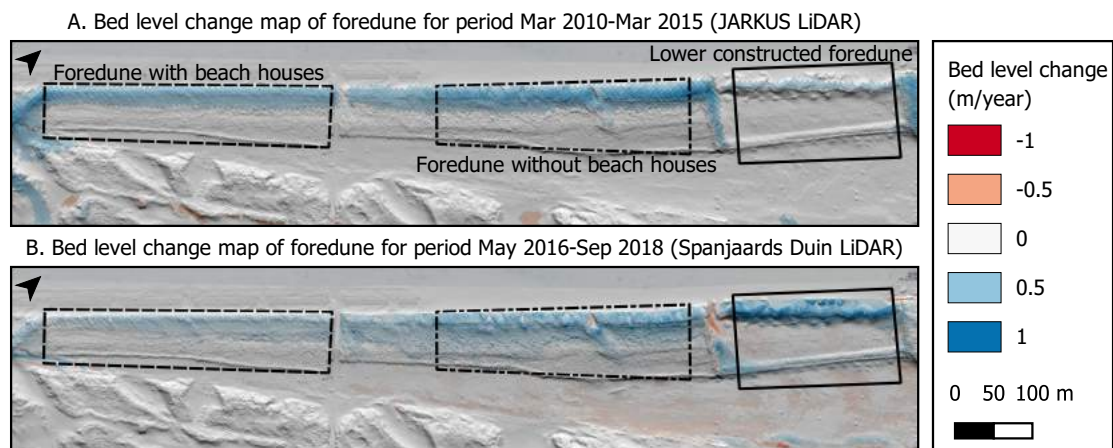


Figure 4.1: Bed level change map of foredune showing JARKUS LiDAR measurements for the period Mar 2010-Mar 2015 (A) and Spanjaards Duin LiDAR measurements for the period May 2016 (T0)-Sep 2018 (T4) (B)

Elevation profiles of the lower constructed foredune directly after construction (period Mar 2009-Mar 2013) show to be stable (Figure 4.2 C). After the planting of vegetation strips on the lower constructed foredune in 2013, this part of the foredune started to grow. Positive bed level changes are observed inside both vegetation strips. In spatial sense, the vegetation strip on the shore side shows higher bed level changes compared to the vegetation strip on the dune valley side. Elevation profiles showed the stabilizing effect of the planted vegetation since cross-shore movement of the foredune was not observed. Furthermore when looking at the bed level change map shown in Figure 4.1 (lower constructed foredune), the sediment deposition patterns follow the curvy pattern of the first (seaward) vegetation strip.

Positive bed level changes are observed for both foredune with and without beach houses located in front (Figure 4.1). Sediment accumulation is observed at the stoss-side of the foredune in the vegetation. Hardly sediment deposition is observed on the lee side. The results of foredune profiles involving beach houses (Figure 4.2 A and B) show a clear difference in morphological development between an area with and without houses on the beach. This difference is most likely caused by the fact that houses block aeolian sediment transport. High accumulation rates were not observed

in front of the houses (sea side), but this could be explained by human activities moving the sand back to the shore to keep the path in front of the houses clean.

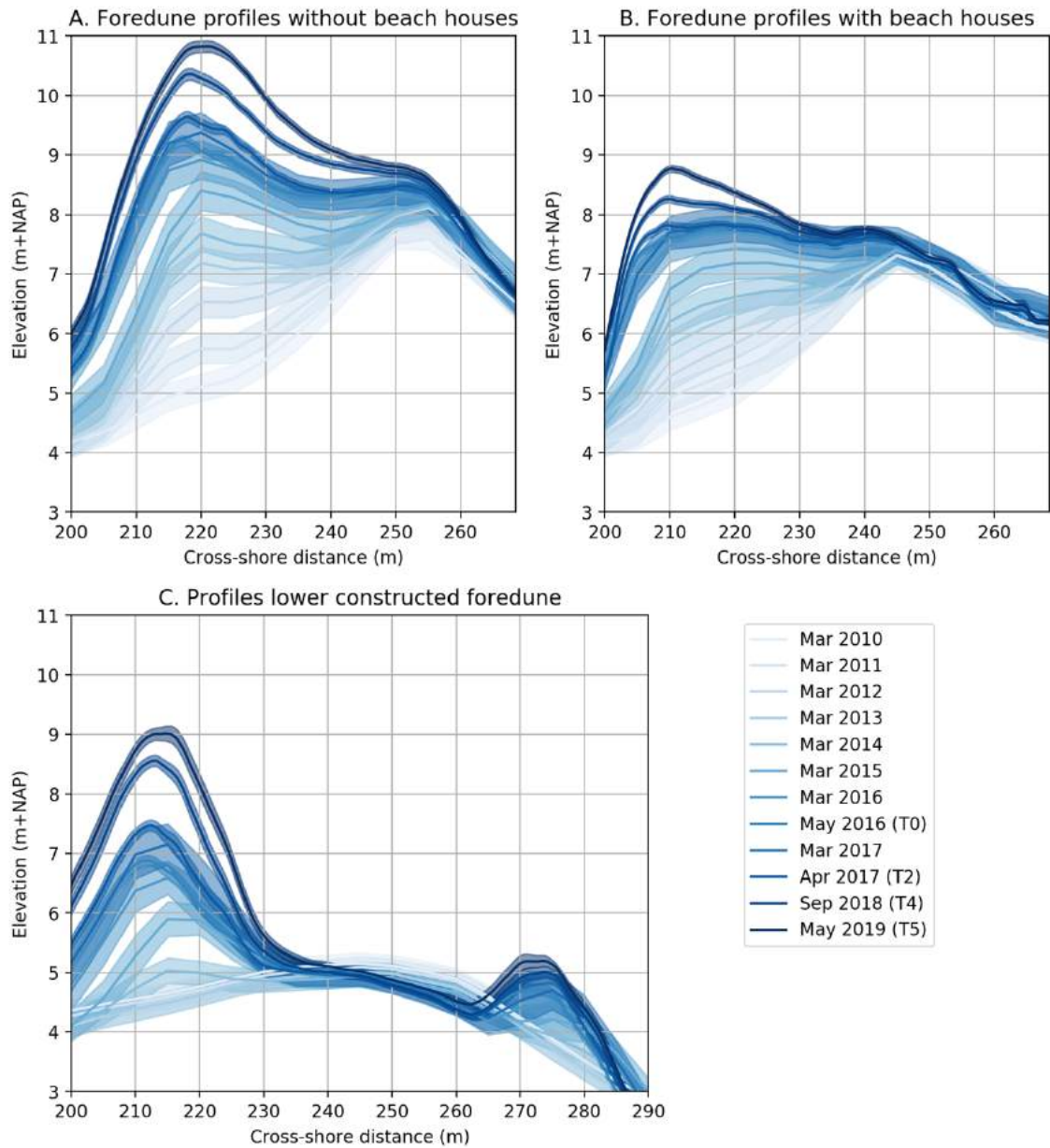


Figure 4.2: Mean foredune profile development including 95% confidence bands for a foredune area without (A) and a foredune with beach houses in front on the beach (B), and the lower constructed foredune used to study the impact of vegetation strips (C). North Sea on the left side of the figure (at $x=0\text{m}$)

4.1.2 Reed bundle fields

Significant accumulation rates for all reed bundle fields are observed in Figure 4.3. Within the field, the sediment deposition is not equally spread. Observed bed level changes within the fields can not be linked to strip densities as defined in Figure 3.5. This deficiency in clarifying patterns could be caused by influences of existing morphology and close located fields, or the (local) multi-directional wind field. Deposition patterns within fields change over time. Figure 4.3 C shows that most of the deposition in field D takes place in the left part. This happens until the reed bundles are fully covered with sand and deposition starts to take place behind the developed hill of sand which is formed in the field which is shown in Figure 4.3 D (field D).

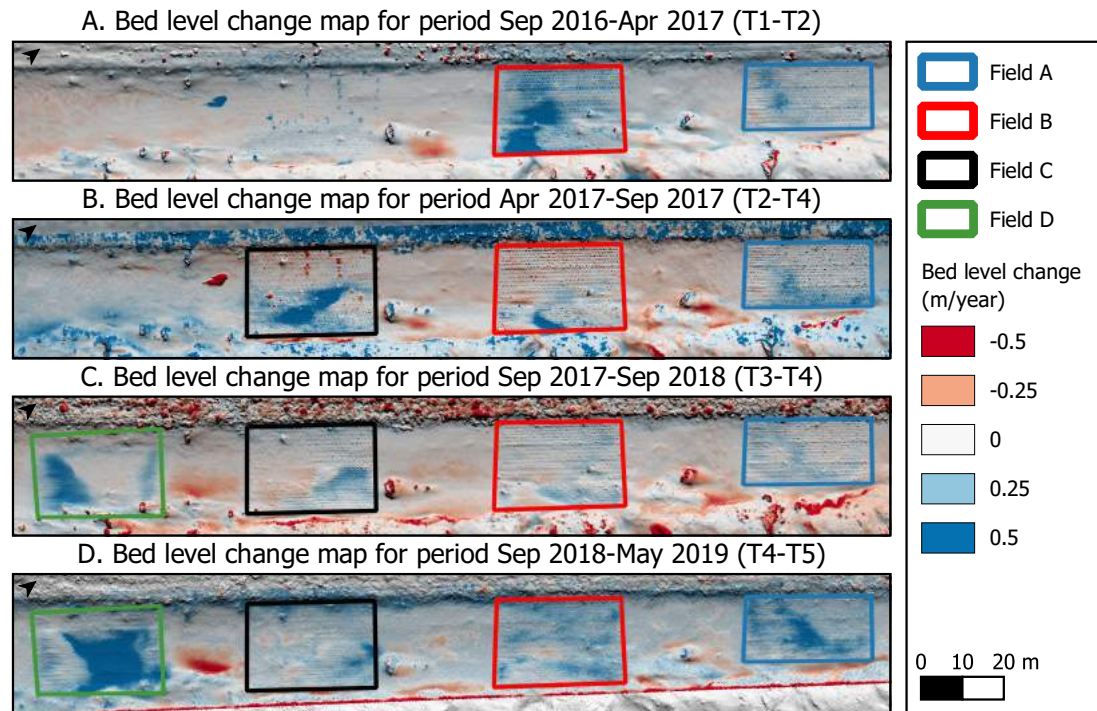


Figure 4.3: Accumulation maps of reed bundle LiDAR measurements showing the reed bundle fields located in the northern valley of Spanjaards Duin. North sea upward of the figures

Since patterns related to reed bundle density were not found the focus was shifted to the total deposition volume for each field. Figure 4.4 shows highest bed level changes in the newest fields located south-west. Beside this, these newest fields are also the most dynamic since the spread in accumulation rates is biggest in comparison to the other fields.

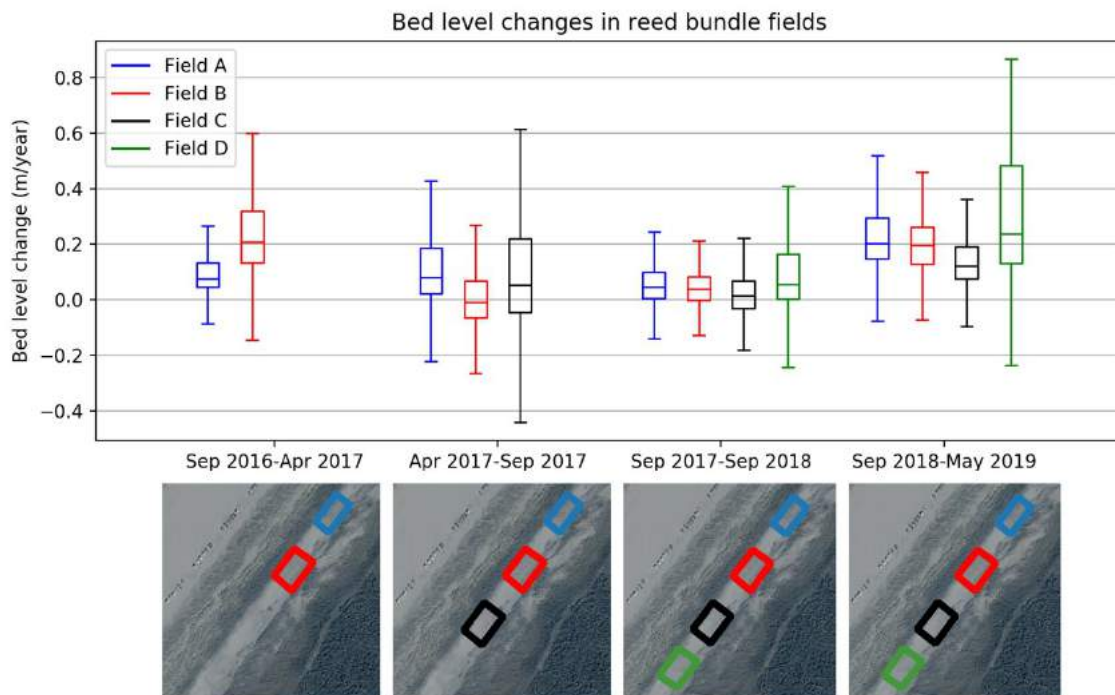


Figure 4.4: Boxplots showing mean accumulation rates for each reed bundle fields

4.1.3 Van Dixhoorndriehoek

Observed erosion patterns can be linked to wind flow patterns classified by Hesp (2002). Inside all blowouts significant erosion rates are observed for all years. Highest erosion rates are observed on the erosional walls. Lower erosion rates are observed inside the blowouts. In the end of a blowout where vegetation starts (depositional lobe), increased deposition rates are observed. Comparing erosion patterns between periods Apr 2017 - Sep 2018 (T2-T4) and Sep 2018 - May 2019 (T4-T5), it was seen that the first period showed more pronounced erosion rates inside the blowouts. Comparing the wind climates for the periods it was shown that the wind climate of the first period was more directed from west (Figure 4.5). With this wind climate wind has more opportunity to blow through the entrance of the blowout.

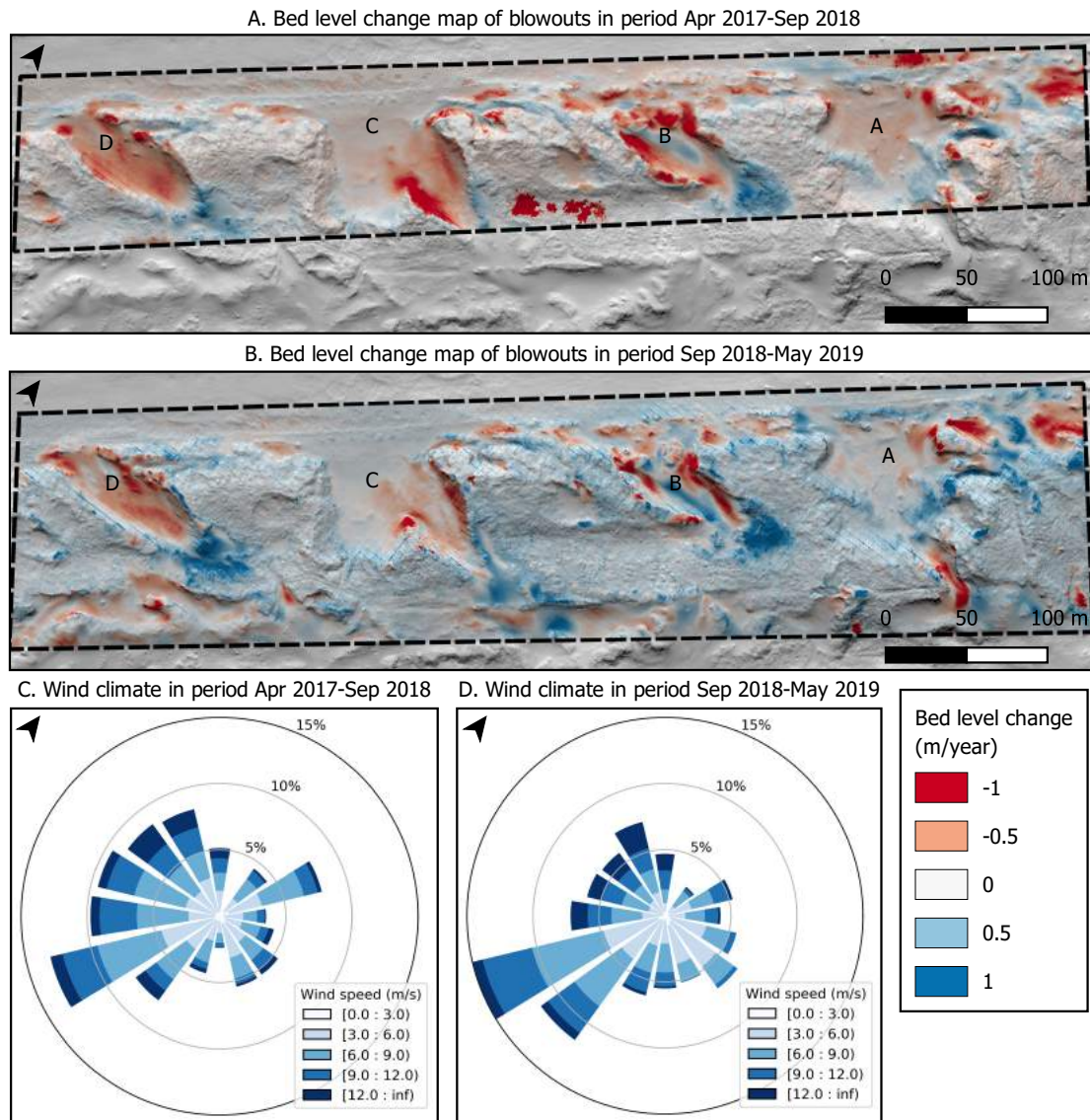


Figure 4.5: Bed level change maps of blowouts located in the Van Dixhoorndriehoek, for the periods Apr 2017-Sep 2018 (A) and Sep 2018-May 2019 (B) including corresponding wind climate (C and D)

4.2 Meso-scale modelling

The modelled aeolian sediment transport direction shows to be different from the mean wind field direction. This difference is largest for years with a multi-directional wind climate (wind events from multiple directions) such as Mar 2011-Mar 2012 and Mar 2014-Mar 2015 shown in Figure 4.6. The maps of other periods are shown in Appendix A. In the period March 2011 – March 2012 highest aeolian sediment transport rates are simulated on the lower constructed foredune (no vegetation) and in the valley behind (dark red area in Figure 4.6 A). Focusing on a period in which vegetation was existing on the lower constructed foredune (Mar 2014-Mar 2015), annual sediment fluxes show lower values most likely caused by the sediment transport reducing effect of the vegetation on the foredune (Figure 4.6 B). In Figure 4.6 B high aeolian sediment transport values are observed in the dune valley behind Slag Vlugtenburg. These high rates are not there in reality and are caused by human management practices (removal of blown sand) around Slag Vlugtenburg which work through in the modelling results.

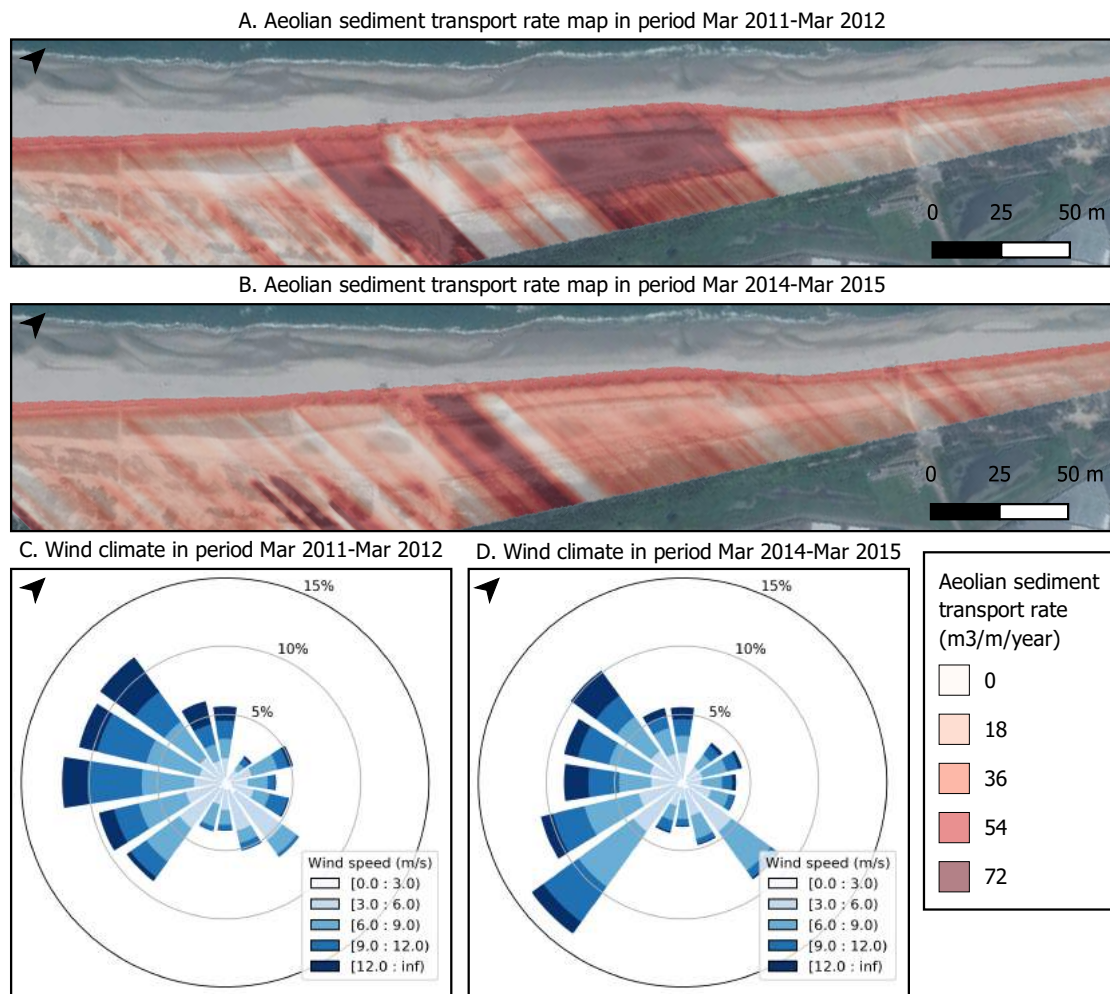


Figure 4.6: Simulated aeolian sediment transport in the meso-scale model for periods Mar 2011-Mar 2012 (A) and Mar 2014-Mar 2015 (B) including corresponding wind climate (C and D)

4.3 Micro-scale modelling

4.3.1 Aeolian sediment transport

Wind events do not contribute equally to the aeolian sediment transport on the foredune and in the dune valley. Figure 4.7 shows the relation between wind event characteristics (magnitude and direction) and the simulated aeolian sediment transport on different parts of the foredune (A, B and C) and in the dune valley (D). It is shown that aeolian sediment transport rates inside the vegetation strips (Figure 4.7 A and C) are determined by wind events perpendicular to the direction of the vegetation strip (wind events from sea and land). Aeolian sediment transport rates on bare parts (Figure 4.7 B and D) show to be much more influenced by wind events with longshore direction (directed from up and below).

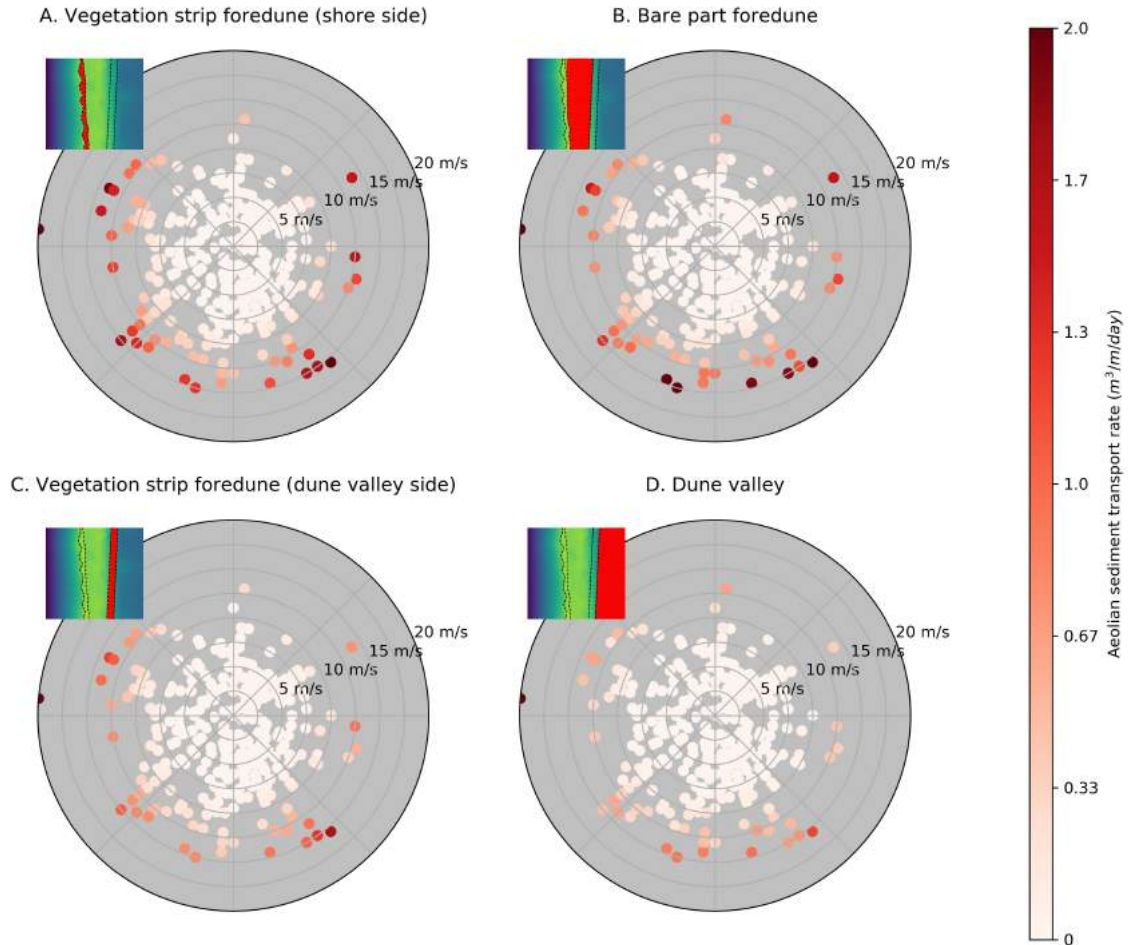


Figure 4.7: Polar plots showing the relation between wind speed, wind direction and the simulated aeolian sediment transport rates in AeLiS for daily events on different parts of the foredune (A, B and C) and dune valley (D). Maps on left top of the figure indicate the analysed area. North Sea on the left side of the figure

Figure 4.8 shows the influence of the foredune and vegetation strips on aeolian sediment transport rates for one high magnitude offshore wind event (21-10-2014, after 235 days in the simulation). This wind event from offshore (magnitude 20 m/s) is also shown in Figure 4.7. The aeolian sediment transport for different vegetation set-ups are plotted for this wind event. The reducing capability of the shore side vegetation strip is visible in figure 4.8 B and C in which a flatten of the curve is observed. The vegetation strip on the valley side (Figure 4.8 D) shows less influence on changing the aeolian sediment transport rate.

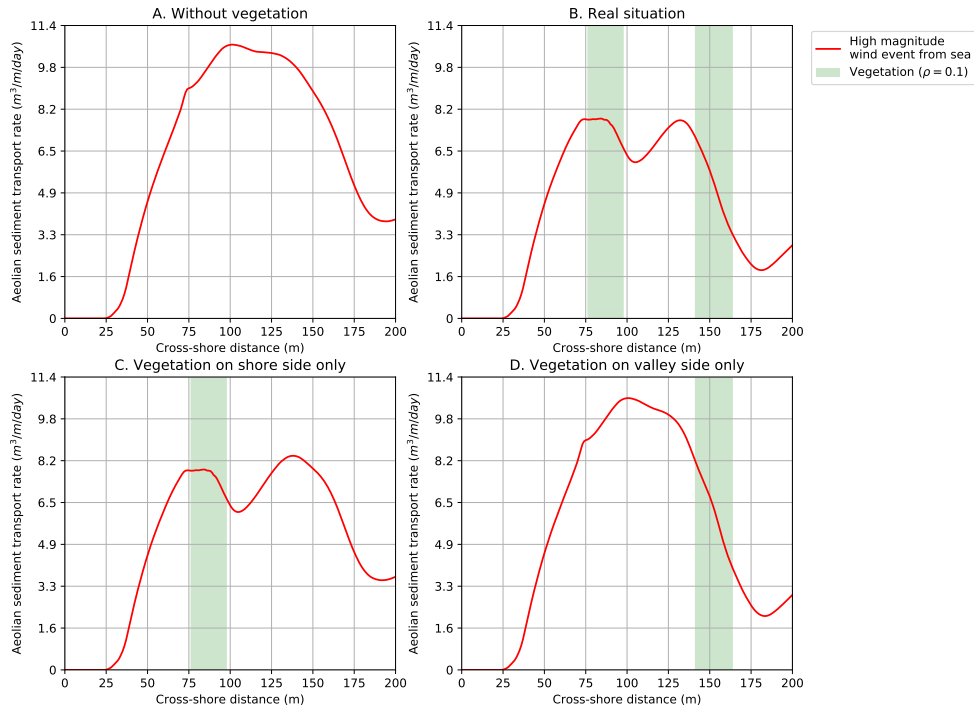


Figure 4.8: Simulated aeolian sediment transport rate in AeoliS across the cross-shore profile (from left to right: beach, foredune and dune valley) for a high magnitude wind event from sea (21-10-2014, after 235 days in the simulation). North Sea on the left side of the figure

When mapping the aeolian sediment transport on an annual scale (meso-scale) using the single events previously described, a deflection of the aeolian sediment transport along the cross-shore profile is observed (Figure 4.9). This deflection can be explained with the relative importance of wind events from different directions (shown in Figure 4.7). The smaller aeolian sediment transport rates on the beach and in the dune valley can be explained by the fetch and aeolian sediment transport reducing capability of vegetation strips shown in Figure 4.8.

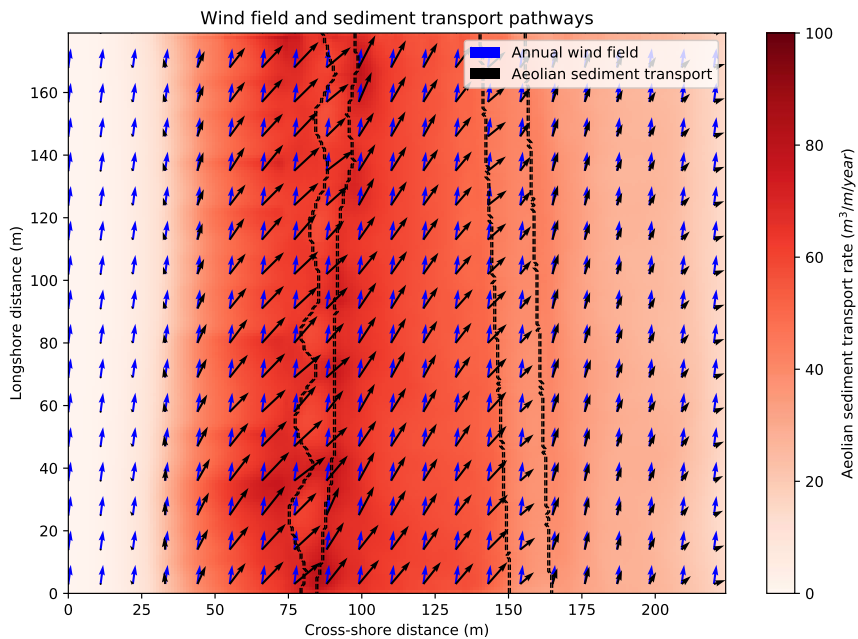


Figure 4.9: Map of simulated aeolian sediment transport in AeoliS on the foredune and in the dune valley including the annual wind field and annual aeolian sediment transport direction. Arrow size indicates the relative magnitude. North Sea on the left side of the figure

4.3.2 Bed level change

Figure 4.10 shows simulated bed levels for all simulations. The simulation of the real situation (Figure 4.10 B) shows the development of the simulated dune profile over a year (monthly interval). The accumulation in the vegetation strip on the valley side is overestimated when compared to the observed foredune profile. The bare part of the foredune (between the strips) is eroding slightly whereas the bed level of the dune valley remains constant. Considering the whole foredune, the foredune is growing with a rate of $40 \text{ m}^3/\text{m}/\text{year}$. A simulation without vegetation (Figure 4.10 A) resulted in a lower accumulating foredune of $14 \text{ m}^3/\text{m}/\text{year}$. The small hump on the stoss side of the foredune showed erosion in this simulation presumably caused by the increasing shear stresses on this bare part of the foredune. Behind the foredune accumulation patterns appear. The simulations with one strip of vegetation (Figure 4.10 C and D) show an accumulation rate of the foredune of 18 and $41 \text{ m}^3/\text{m}/\text{year}$ respectively. The latter result (D) showed even an increase the accumulation rate compared to the real situation (B).

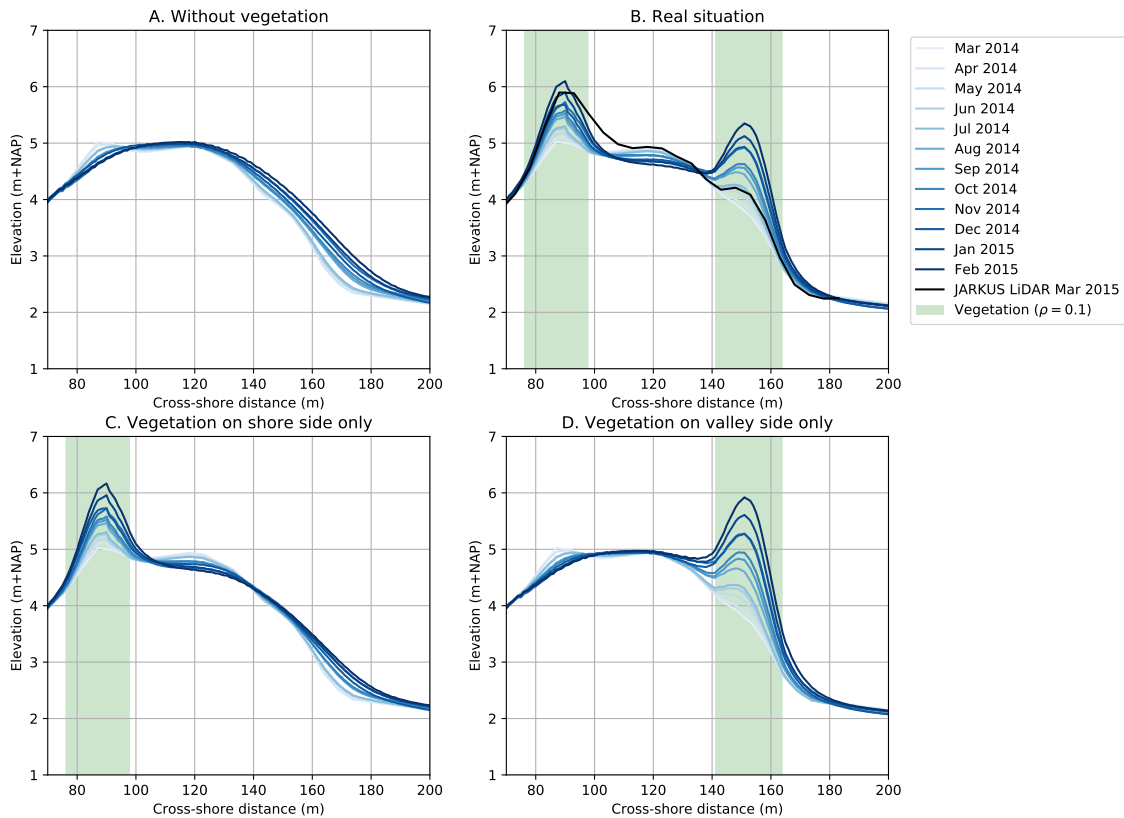


Figure 4.10: Simulated mean foredune profiles in AeoliS for different vegetation scenarios: without vegetation (A), real situation as in Spanjaards Duin (B) and with only one vegetation strip on shore side (C) and dune valley side (D). The simulated profile of Mar 2014 is the initial model state and corresponds with JARKUS LiDAR Mar 2014. North Sea on the left side of the figure

4.3.3 Sediment grain size distribution

Aeolian sediment transport changes the initial sediment size distribution (sediment sorting). In the first 15 days of the simulation, most of the sediment sorting took place. On the bare part of the foredune and in the dune valley results show the increased dominance of the largest sediment fractions, especially shells (6 mm) (Figure 4.11 A and B). Inside the vegetation strips (in the green area) the opposite effect occurs where deposition of fine sediment results in a sediment size distribution dominated by small particles. When looking at the sediment mass in the bed surface layer (Figure 4.11 C, D, E and F) the changes in mass of different particles sizes are in line with the observations from figure A and B. When comparing bare areas (C and E) with vegetated areas (D and F) the exact opposite development pattern is observed. Counter-intuitively the mass of the biggest particles show dynamic behaviour too (decreasing mass in vegetation, increasing mass on bare parts). This dynamic behaviour is not caused by deposition or erosion of large particles, but can be explained by the model property of exchanging sediment between the bed surface layer and the bed composition layers after a time step (explained in Figure 3.8). Figures 4.11 B and C show the increase of the weight of the big fractions of sediment in the top layer on the bare part of the foredune.

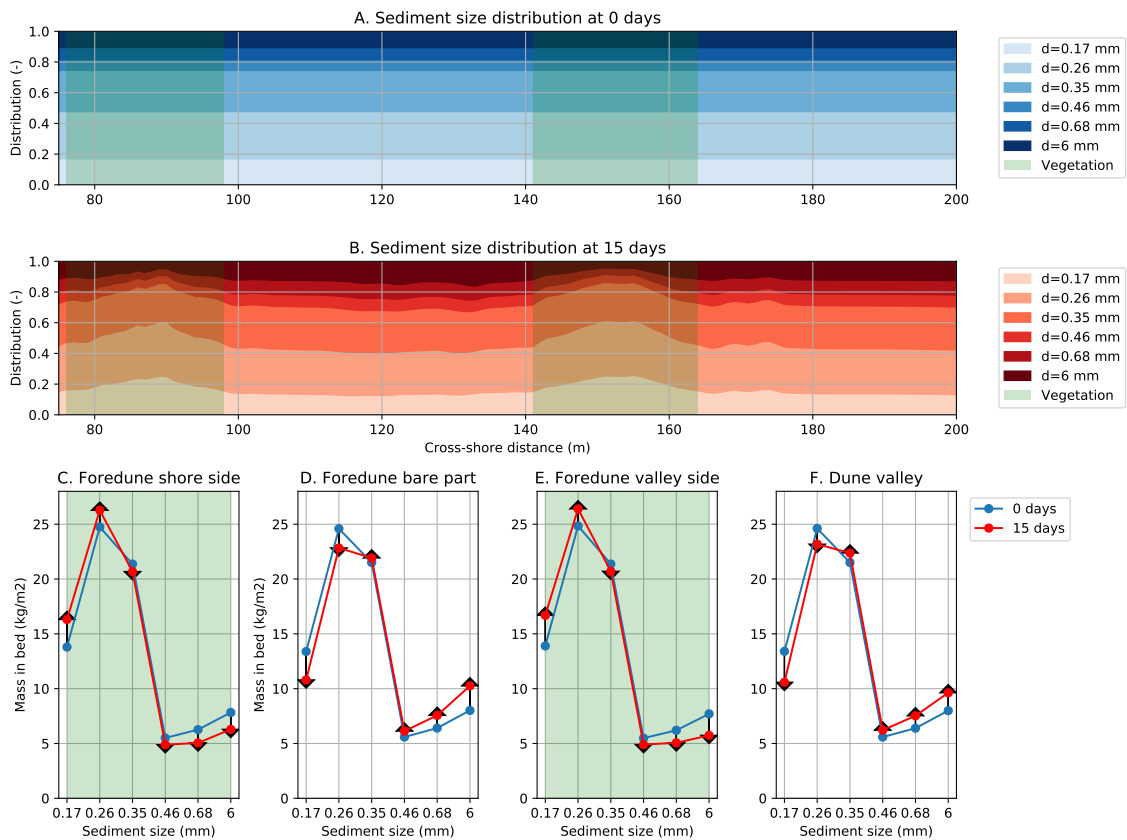


Figure 4.11: Simulated sediment grain size distribution in AeoliS showing the initial (A) and the sediment grain size distribution after 15 days (B). The changing mass in the bed surface layer is shown for the vegetated parts (C and E) and the bare parts (D and F). The black arrow indicates the direction of change

Chapter 5

Discussion

The results showed aeolian sediment transport pathways and the interactions between aeolian sediment transport, bed level change and the sediment grain size distribution in Spanjaards Duin. The meaning and significance of the results are discussed in this chapter.

5.1 Aeolian sediment transport

Bed level change maps showed to be an effective way to identify possible aeolian sediment transport pathways in Spanjaards Duin. This was shown by the transport pathway in the foredune (Figure 4.1 B) and erosion patterns in blowouts located in the Van Dixhoorndriehoek (Figure 4.5). Identifying the blowouts as a significant sediment source should be a rushed statement since eroded sediment is deposited locally in the vegetation surrounding the blowouts. However, this does not alter the fact that in case of a wind from land, sediment will be transported from the blowout into the dune valley. It was attempted to link the wind climate to the erosion rates in blowouts. Figure 4.5 showed that high wind events blowing through the entrance of the blowouts resulted in higher erosion rates. However, no statistical evidence for this link was found. Beside this, other factors than wind influence the erosion rate in blowouts too. The dryness of the surface is expected to be the most important factor influencing the erosion of the surface (Aggenbach et al., 2018). Aggenbach et al. (2018) stated that blowouts with an orientation South should show highest erosion rates since exposure by sun drying is highest. This factor taking into account the soil moisture in the surface should not be depreciated in this analysis since periods covering different seasons (different soil moisture contents) were compared.

A meso-scale modelling approach was used to calculate aeolian sediment transport on an annual basis. The model is entirely based on monitoring data (bed levels and wind) and therefore limitations in the bed level data work through in results of the model (further elaborated in Section 5.2). Therefore, modelled aeolian sediment transport rates in the Van Dixhoorndriehoek and around Slag Vlugtenburg should be interpreted with some caution because human interventions influenced the model results. Beside this, the model describes behaviour of the system on a meso-scale level. Therefore the model is an added value to explain the qualitative behaviour of aeolian sediment transport in coastal dune and dune valleys, but cannot be used to quantify the abiotic influence of sand blasting impacting natural vegetation development. For that, a micro-scale modelling approach using shorter time intervals is needed.

Aeolian sediment transport was modelled across a foredune on a micro-scale in AeoliS. Not all wind events contributed equally to aeolian sediment transport rates on the foredune and in the dune valley (Figure 4.7). Many low wind speed events resulted in zero aeolian sediment transport which can be explained by the fact that the threshold shear velocity is not reached and therefore the sediment transport capacity is not reached (Bagnold, 1937; Sherman & Li, 2012). The results of aeolian sediment transport modelling were compared to measured aeolian sediment transport rates on a foredune of the Sand Motor located 5km North of Spanjaards Duin (Vertegaal et al., 2016). Aeolian sediment transport rates were measured using sand traps placed along a transect on the foredune. Results showed that sediment transport across the foredune was event-driven. Especially winds from sea were responsible for high sediment transport rates. These measured results are in agreement with results presented in Figure 4.7. Figure 4.8 shows the influence of the foredune on aeolian sediment transport rates in case of a wind event from sea. Vegetation

strips showed to lower the aeolian sediment transport rate (comparing Figure 4.8 A with B). The quantification of the aeolian sediment transport rates should be interpreted with some caution, because the aeolian sediment transport rate was calculated in AeoliS by the wind speeds times the sediment concentration in air. A convenient approximation of the aeolian sediment transport rate should be using the particle speed instead of the wind speed, since the wind speed is higher than the sediment particle speed. Drag forces act on the particles which slow them down and gravity forces cause particles to show saltation behaviour (Section 2.1.3) which does not entirely follow the wind flow direction (Sauermann et al., 2001). For these reasons the sediment transport rates are overestimated in this version of AeoliS. Beside this model limitation, the model assumes no aeolian sediment transport rate on the landward boundary. In case of a wind from land, no sediment would enter the system. In case of high magnitude events with wind from land it is expected that aeolian sediment transport rates would enter the system in reality.

Results between different modelling approaches showed differences in annual aeolian sediment transport pathways (Figure 4.6 and 4.9). This difference can be explained by the fact that the meso-scale approach only uses the wind climate for defining the annual aeolian sediment transport direction, while the micro-scale approach incorporates all the processes related to spatial elements such as vegetation and moisture. Because of this, the micro-scale modelling approach benefits the meso-scale modelling approach. The calculated sediment fluxes from AeoliS could be used to explain the behaviour of the system, however are quantitatively not reliable enough to determine the sandblasting stresses on vegetation.

5.2 Bed level change

The quality (resolution and error) of the JARKUS LiDAR dataset was good enough to describe the morphological development of Spanjaards Duin. However abiotic conditions in terms of bed level changes could not be derived since the resolution (5 m) and error (0.21 m) was expected to be too high when focusing on vegetation (Section 3.1.1). The Spanjaards Duin LiDAR was more suitable for defining the abiotic conditions focusing on bed level changes since the error (0.04 m) was smaller in comparison with the maximum burial rate for dry grey dune vegetation (0.1 m), shown in Table 1.1. In the bed level data atypical erosion patterns were observed (Appendix A), but could be explained by human management practices. Examples were: digging out of blowouts, lowering of the dune valley and human influences around Slag Vlugtenburg. The observed positive bed level changes on the foredune showed to be dominated by vegetation and not by morphology (Figure 4.2 C). Accumulation rates were observed just inside the vegetation and not behind the crest as described in section 2.3.2 based on Walker and Nickling (2002). This minor influence of the morphology could be explained by the fact that the foredune consists of relatively gentle slopes or the dominance of Marram grass as a dune building species (Zarnetske et al., 2012). The observed accumulation rates inside the Marram Grass on the foredune (Figure 4.2 C) were within expected ranges described in literature. Marram grass can cope up with an accumulation rate of 1 m/year (Huiskes, 1979) or even 2 m/year (Baas & Nield, 2010). In the case of a foredune with beach houses positioned on the beach less morphological development of the foredune was observed (Figure 4.2 B). However the influence of beach houses on aeolian sediment transport in the dune valley seemed minor. This result is in agreement with de Klerk (2019) who states that beach buildings influence aeolian sediment transport only locally.

AeoliS showed to be able to reasonably simulate bed level changes as observed in monitoring data (Figure 4.2 and Figure 4.10 B). However, in the vegetation strip on the valley side the simulated bed level change was overestimated compared to LiDAR data. This disagreement between model and reality could be explained by a too high supply of sediment to the foredune in the model. A second more justified explanation could be that AeoliS does not simulate the process of counter turbidity of flow behind the foredune (Figure 2.3 C) which mobilizes sediment particles and prevent them from being deposited. This is in agreement with the foredune simulation without vegetation (Figure 4.10 A). A stable profile is shown which is in agreement with observations shown in Figure 4.2 C, but in the valley side accumulation patterns are shown which were not expected. The bed level changes simulated in AeoliS showed to follow a persistent trend over the year (e.g. inside vegetation increasing trend for the whole year). Therefore observations from data (Spanjaards Duin LiDAR only) were expected to cover all information about bed level changes in Spanjaards Duin.

5.3 Sediment size distribution

The sediment size distribution showed dynamic behaviour in which vegetation showed to be an important factor in determining the sediment size distribution of the bed surface layer (Figure 4.11). On the bare areas sediment sorting and the emergence of non-erodible layers resulted in a stabilized bed surface layer dominated by rough particles (Figure 4.11 D and F). This result is in agreement with several studies focusing on the development of nourished beaches in The Netherlands on the island of Ameland (Van der Wal, 2000) and the Sand Motor (Hoonhout & de Vries, 2017). Beside this, field observations shown in Figure 5.1 confirm this result.



Figure 5.1: Emergence of non-erodible layers (shells) on the bare part of the northern foredune between vegetation strips (A), and in the southern valley (B). Photos taken on 12-03-2020

Chapter 6

Conclusion

This research aimed to increase the quantitative knowledge of the interaction between aeolian sediment transport and abiotic conditions for natural vegetation development in engineered coastal dunes and dune valleys. The sub-questions and main question are answered in this chapter.

1. Which aeolian sediment transport pathways exist in Spanjaards Duin?

The annual aeolian sediment transport pathways are controlled by high magnitude wind events. The impact of each wind events differs per location and is highly influenced by the foredune. The foredune including its vegetation (Marram grass) is an important element in reducing aeolian sediment transport in the dune valley, regardless of beach houses located in front of the foredune. The influence of the foredune is the cause that annual aeolian sediment transport pathways are different for the foredune and the dune valley. Cross-shore directed sediment transport happens on the foredune, and (lower rate) longshore directed transport happens through the valley. To model transport pathways, a micro-scale modelling approach is favored over the meso-scale modelling approach.

2. What is the impact of aeolian sediment transport on the bed level change in Spanjaards Duin?

Bed level changes in Spanjaards Duin are primary controlled by vegetation and the sediment grain size distribution. Accumulation takes mostly place on the foredune. Accumulation caused by Marram Grass or artificial reed bundles is too large to reach favourable bed level changes for target habitats. Wind exposure on parts without vegetation causes the bed to erode. The changing grain size distribution is responsible for stabilizing the bed. Favourable abiotic conditions in terms of bed level change are reached in the dune valley.

3. What is the impact of aeolian sediment transport on the sediment grain size distribution in Spanjaards Duin?

Aeolian sediment transport impacts the sediment grain size distribution by sorting the sediment. The impact differs between areas with and without vegetation cover. Inside vegetated areas sediment sorting causes a change of the sediment grain size distribution to a distribution dominated by small particles. On areas without vegetation the exact opposite effect appears in which large particles become dominant in the distribution. Applied to Spanjaards Duin, these large particles are shells which form a non-erodible layer near the surface. The sediment size distribution of layers below (sheltered by the bed surface layer) are expected to maintain its original distribution of dredged sand.

What is the impact of aeolian sediment transport on abiotic conditions for natural vegetation development in engineered coastal dunes and dune valleys?

Aeolian sediment transport impacts the abiotic conditions by changing characteristics of the surface (bed level, grain size distribution) and the air (sand blasting). Abiotic conditions showed to largely influence each other (answer in sub-question 2 and 3), and never reach favourable conditions for all factors. In engineered coastal dunes and dune valleys such as Spanjaards Duin it was shown that two factors played a key role in lowering the impact of aeolian sediment transport on abiotic conditions. 1) Marram grass: functioning as a bodyguard to reduce aeolian sediment transport in the dune valley. 2) Nourished sand: which contains shells and functions as a stabilizing effect for the bed level in the dune valley. Beside this, the shells prevent the dune valley from being a sediment source.

Chapter 7

Recommendations

The recommendations are split up in three different sections. The first section elaborates on the construction of Spanjaards Duin, the second section focuses on management practices which can be taken in the short-term and the third section provides recommendations for future study suggesting ideas for biophysical modelling.

Design of moist dune slack valleys

The construction of dune valleys suitable for moist dune slack vegetation needs careful attention. Constructing the bed level too high result over time in a stabilized (slightly eroding) bed dominated by shells. It is uncertain if these dominance by shells at the surface impede germination of seeds. It is certain that the stabilized bed is too high for development of moist dune slack vegetation. This knowledge was already used and resulted in an interference in January 2019, lowering the bed level of the dune valley (Arens et al., 2018). If the bed level was initially constructed too low the appeared dune lakes (also existing after the interference) would capture sediment and the bed level would naturally increase to the suitable bed level for the development of moist dune slack vegetation.

Management practices

It is aimed to reduce aeolian sediment transport rates (also often defined as sediment fluxes) in the dune valley. Planting Marram grass or constructing reed bundle fields is an effective measure to protect areas by reducing aeolian sediment transport, however should not be used in the target habitat areas to enhance vegetation development, since accumulation rates become too high. Planting Marram grass is recommended above reed bundles because of its properties of growing with the positive bed level change. For defining the location of planting to avoid sand blasting it is important to incorporate all wind events contributing to aeolian sediment transport on the location. In the dune valley this means that wind events from south-west are most important (aeolian sediment transport through the valley). The planting of Marram grass in the valley shown in Figure 1.2 is expected to be effective in protecting the area north-east of it from sand blasting. Aeolian sediment transport will also decrease when sediment supply into the valley is limited. This can be achieved by limiting all supply of sand to the dune valley by planting Marram grass or placing reed bundles. This should be done in the eroding aeolian sediment transport pathway identified in Figure 4.1. Based on LiDAR data no evidence was found of sediment entering the dune valley via blowouts (Van Dixhoorndriehoek) and the southern entrance of the dune valley. However, this does not mean that these borders can be excluded as potential sediment sources. Therefore it is recommended to perform aeolian sediment transport measurements.

Biophysical modelling

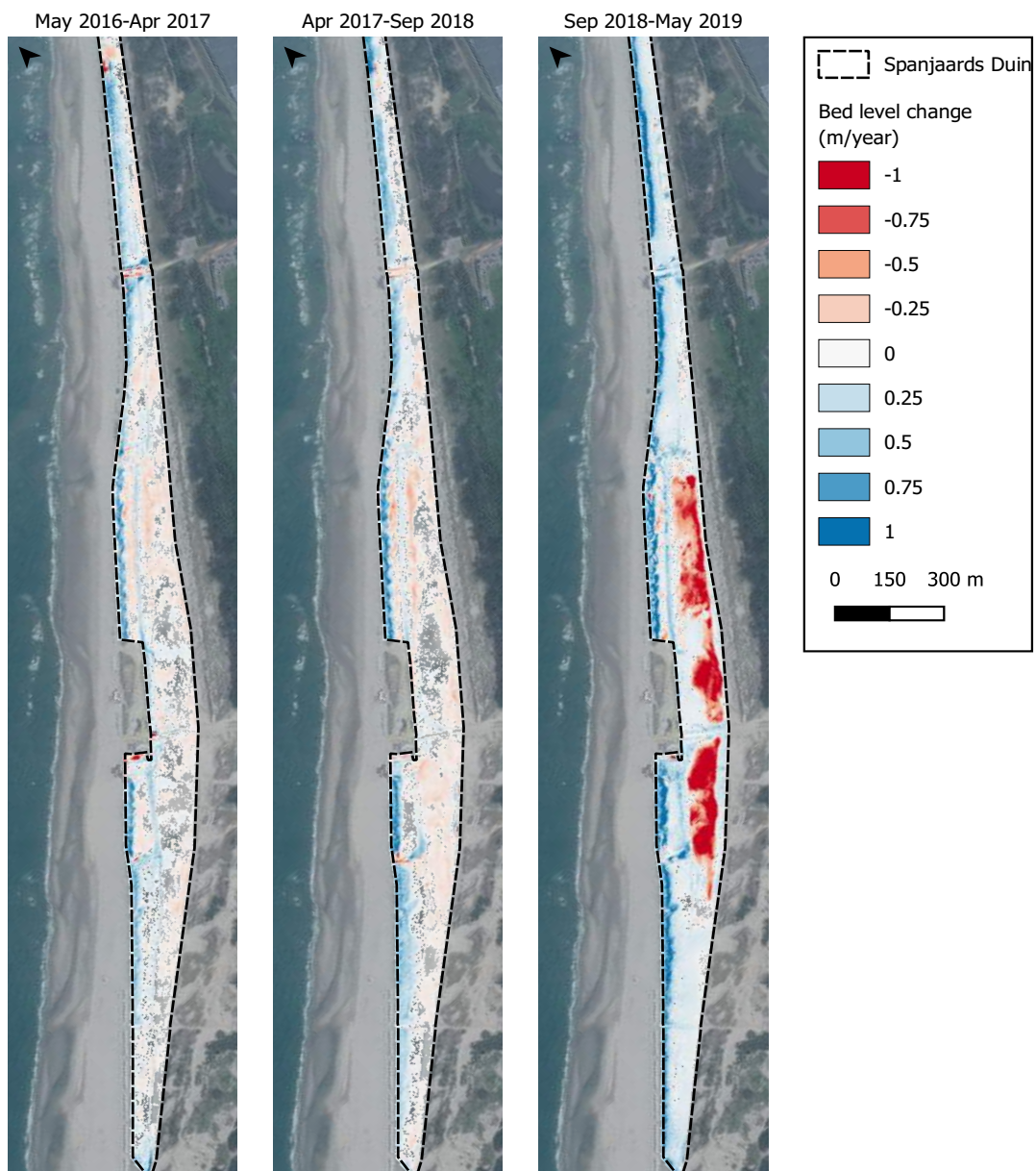
This research focused on the interaction between aeolian sediment transport and the abiotic conditions. To bring knowledge about nature development in these engineered coastal dunes and dune valleys to a next step the biophysical interaction between vegetation and abiotic conditions should be defined. It is recommended to model the vegetation development by using a window of opportunity approach invented by Balke et al. (2013). A window of opportunity is a disturbance-free

period of a defined minimum duration that allows for vegetation to establish. This research aimed to increase knowledge of these disturbances (abiotic conditions). However to take knowledge about vegetation development in Spanjaards Duin to a next step, tipping points are needed. Tipping points can be explained as the threshold value at which a certain abiotic factor cause damage to vegetation. Questions should be asked as: until which aeolian sediment transport rate is the development of target habitats not affected? It is recommended to include: aeolian sediment transport (sand blasting), bed level change, sediment grain size distribution and as extra (not studied in this research): (seasonal) flooding and soil moisture content.

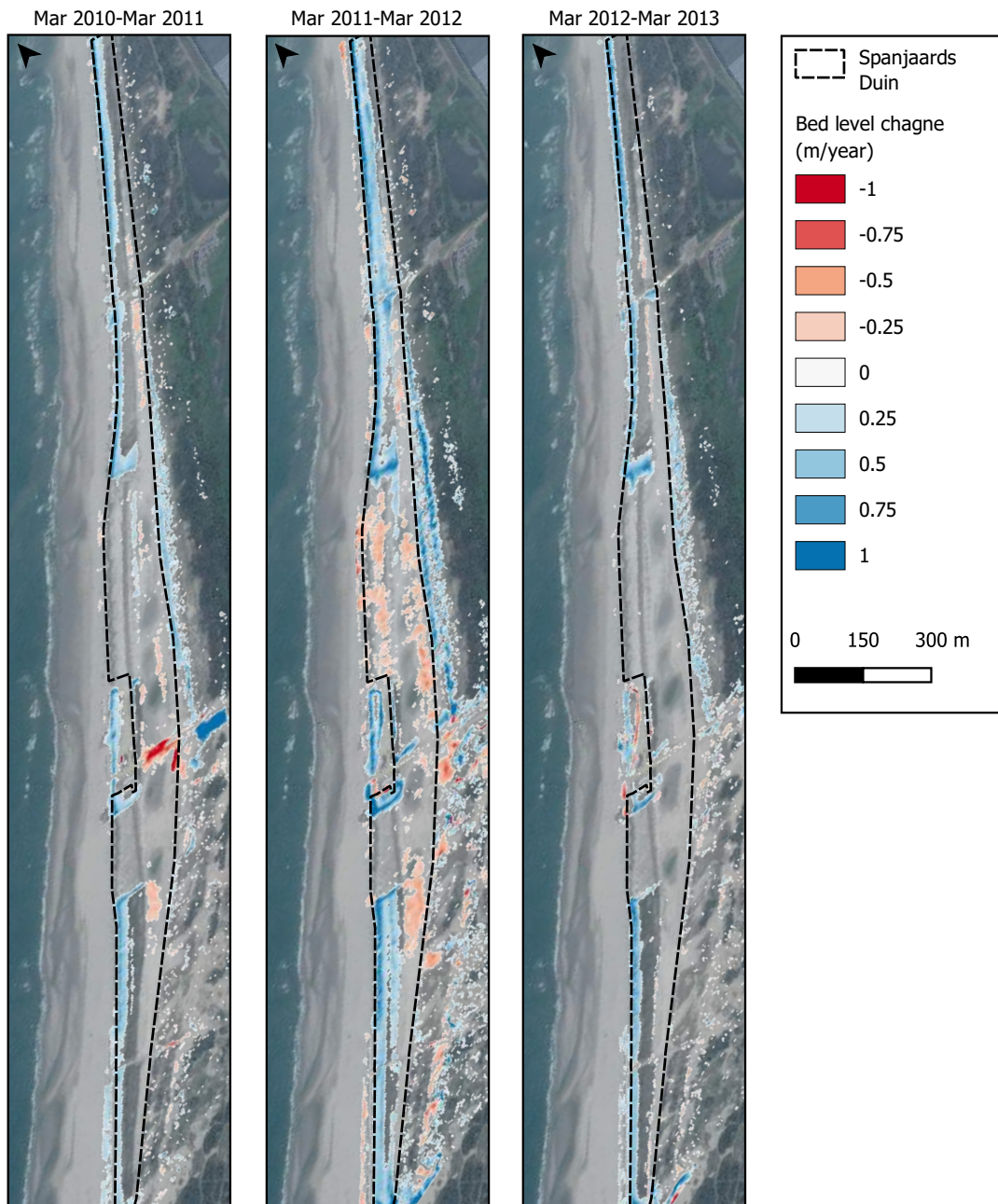
Appendix A

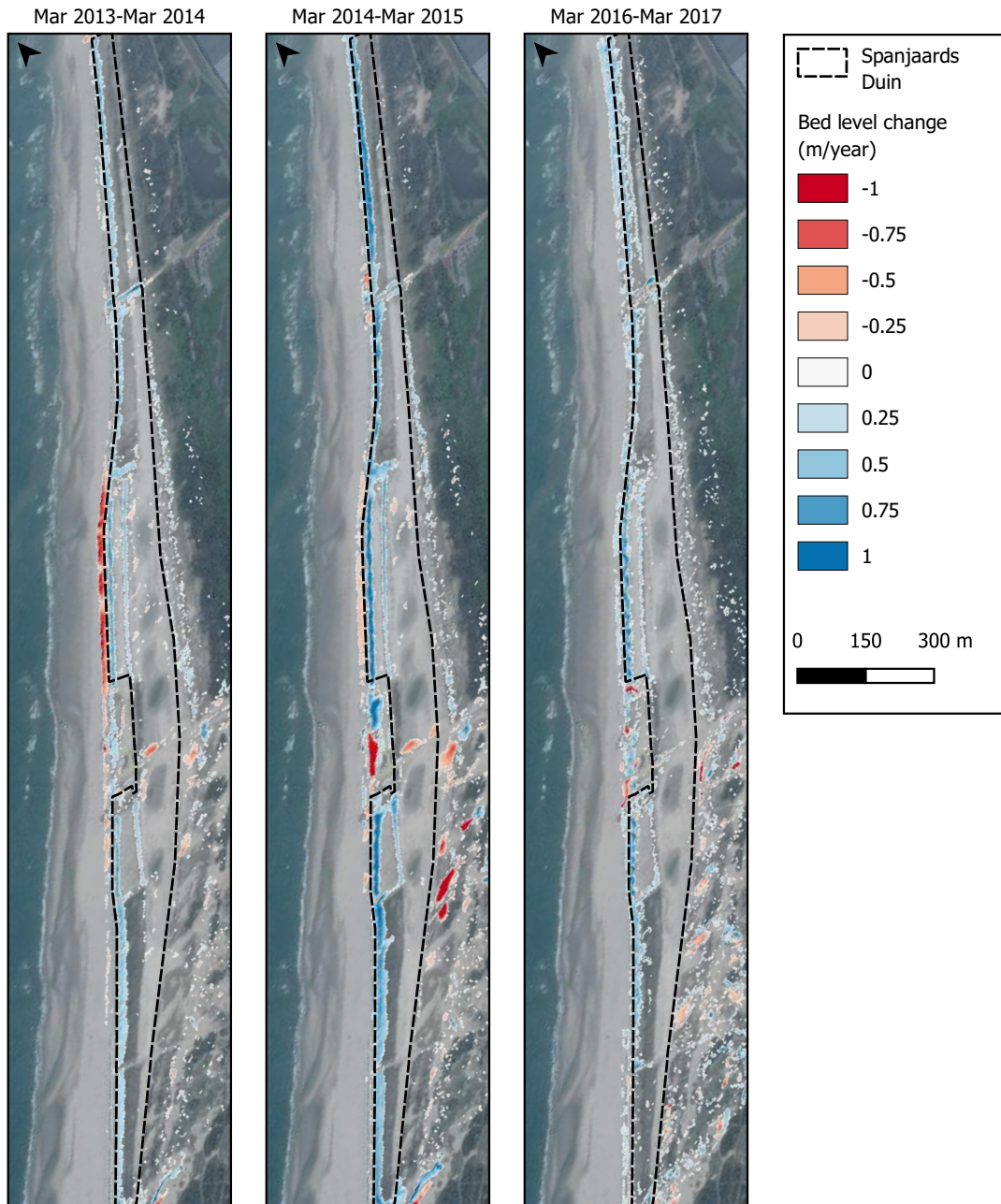
Maps

Bed level change maps Spanjaards Duin LiDAR

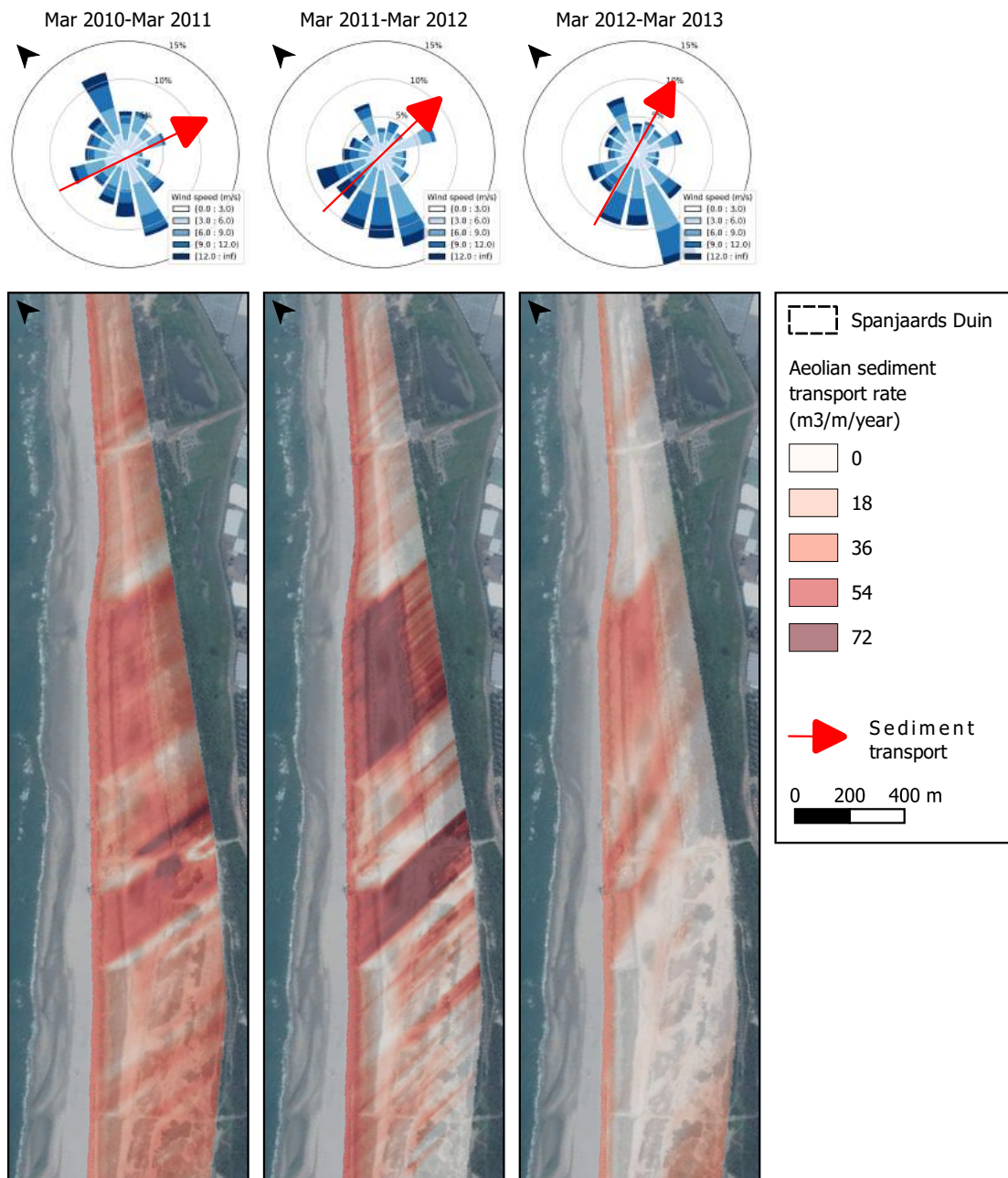


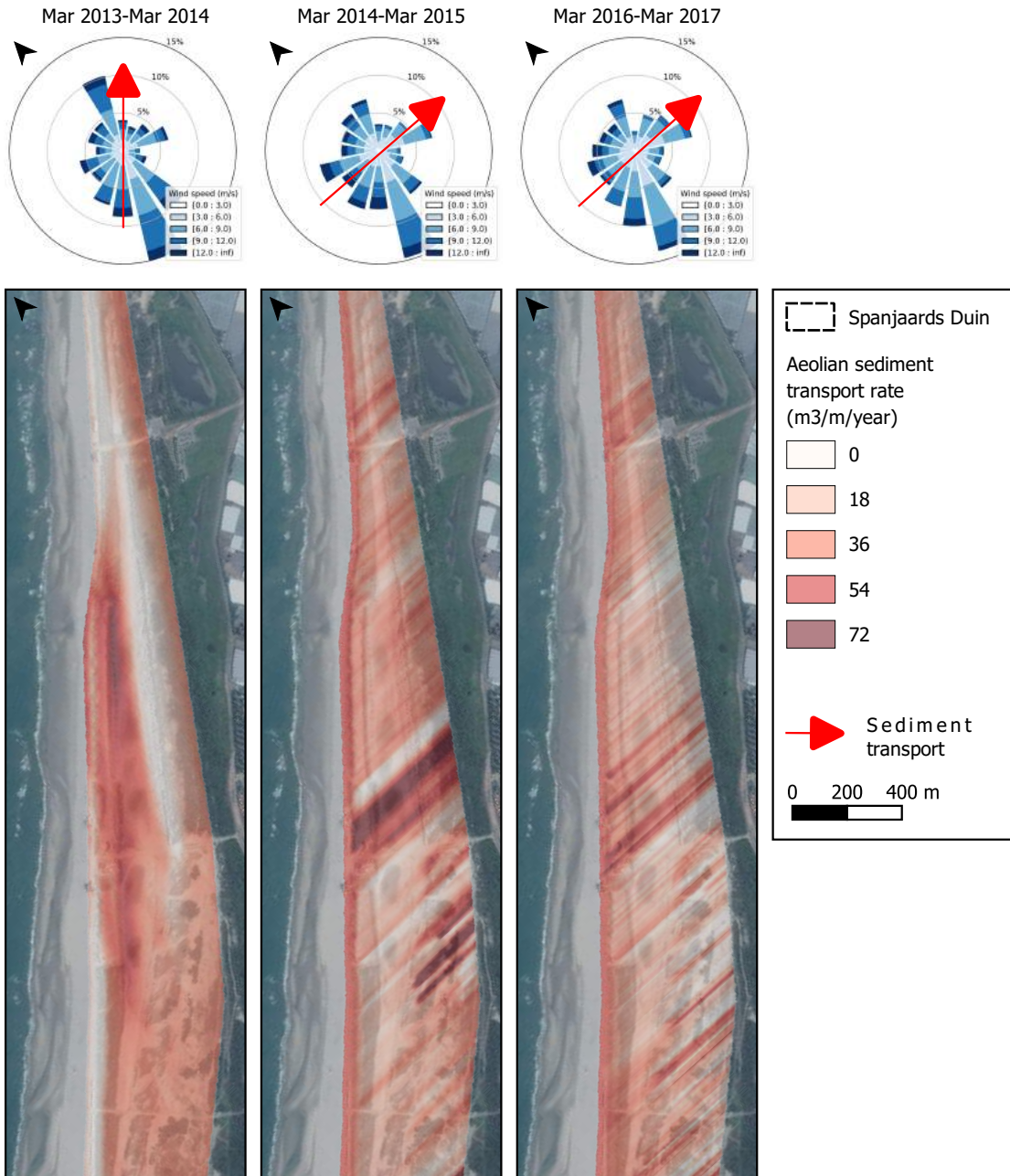
Bed level change maps JARKUS LiDAR





Meso-scale aeolian sediment transport





Appendix B

AeoLiS model description

AeoLiS is a 2DH aeolian sediment transport model in development. A first version was developed by Hoonhout & de Vries (2016). van Westen (2018) extended AeoLiS by adding dune development processes from a different model called CDM and vegetation germination and lateral expansion processes were implemented from DUBEVEG (Keijsers et al., 2016). Model development is currently taking place at Deltares by extending the model of van Westen (2018) by aeolian sediment transport for multiple sediment fractions for multi directional flow. A first version was used in this study. A qualitative explanation of most important processes is given in this appendix.

Aeolian sediment transport

Aeolian sediment transport in AeoLiS is based on the transport formula of Bagnold (1937) shown in Equation 2.2. The sediment transport capacity or equilibrium concentrations calculated with this formula are often not reached because of limiting factors and spatial variability in sediment transport capacity (Roelvink & Costas, 2019). The actual sediment transport rates or sediment concentrations are calculated using an advection equation:

$$\frac{\partial c}{\partial t} + u_z \frac{\partial c}{\partial x} = E - D \quad (\text{B.1})$$

Where c represents the actual sediment concentration, t and x denotes time and space. E represents the erosion and D represents the deposition. The erosion minus deposition (sediment entrainment) can also be approached as the difference in equilibrium concentration and actual concentration, maximized by the maximum amount of sediment available (Hoonhout & de Vries, 2016):

$$E - D = \min\left(\frac{\partial m_a}{\partial t}, \frac{c_s - c}{T}\right) \quad (\text{B.2})$$

Where m_a represents the available sediment on the bed, c_s is the saturated sediment concentration calculated from the transport capacity calculated from Equation 2.2. T represents an adaptation time-scale of order 1 s (Hoonhout & de Vries, 2016).

Multiple layers and fractions

AeoLiS defines three different types of vertical layers. The top layer on the surface is called the bed surface layer, the layers below are defined as bed composition layers. Below the bed composition layer a base layer is situated which contains an unlimited amount of sediment. The bed surface layer is the only layer which interacts with the wind, therefore sediment only leaves a grid cell via the bed surface layer. When sediment is picked-up from a grid cell sediment is repleted from the bed composition layer below. Vice versa when sediment is deposited, sediment is excessed to the bed composition layer below. A visualization of this is shown in Figure 3.8. In AeoLiS, multi fractional sediment transport is simulated. The sediment transport for each fraction is calculated separately. Each sediment fraction has a different threshold from being transported. Therefore sediment sorting takes place. On a bare surface sediment sorting results to a sediment size distribution with more rough particles, all finer particles are transported.

Wind field

Wind blowing over a surface is perturbed caused by morphology changes. The perturbation of the wind field is implemented by the analytical perturbation theory for turbulent layer flow (Weng et al., 1991). This perturbation theory calculates a shear stress perturbation based on perturbations in the morphology. Flow separation behind the top of the dune is implemented with a separation bubble (Sauermann et al., 2001). The separation bubble represents the separating streamline. The shape of the separating bubble is a third-order polynomial. When slopes become too steep AeoliS applies avalanching. Slopes are too steep when they are bigger than static response angle. Slopes avalanche to the dynamic response angle. Avalanching consequences into sediment transport. This transport rate is calculated following Kroy et al. (2002).

Vegetation

The shear stress acting on the sand is reduced by the presence of vegetation. This shear stress reduction is calculated based on Raupach et al. (1993). Raupach et al. (1993) uses a stress partitioning approach to parametrize the shear stress on a surface with vegetation in terms of a shear stress acting on a bare surface. Vegetation growth is based on DUBEVEG (Keijsers et al., 2016) and is specified in AeoliS using a vegetation growth rate (V_{veg}) and a constant which incorporates the influence of burial (γ_{veg}).

Swash zone processes

Hydrodynamic processes are responsible for sediment supply to the beach. Tides and wave run up are implemented in AeoliS which results in occasionally flooding of the swash zone. In the period of low tide the swash zone is not flooded and sand can be transported to the beach and foredune. In case of high tide grid cells in the swash zone are flooded. Hydrodynamic sediment supply is implemented in the model using a rule stating that the bed level of a flooded grid cell is changed (increased) to the initial bed level. Beside this hydraulic mixing is implemented by changing the sediment size distribution to the original one (Hoonhout, 2019).

Bibliography

- Aggenbach, C., Arens, S., Fujita, Y., Kooijman, A., Neijmeijer, T., Nijssen, M., Stuyfzand, P., van Til, M., van Boxel, J. & Cammeraat, L. (2018). *Herstel grijze duinen door reactiveren kleinschalige dynamiek*. Vereniging van Bos- en Natuurterreineigenaren (VBNE).
- Arens, S., Baas, A., Van Boxel, J. & Kalkman, C. (2001). Influence of reed stem density on foredune development. *Earth Surface Processes and Landforms*, 26(11), 1161–1176. doi:10.1002/esp.257
- Arens, S., Beekman, W., Caljé, R., van den Heuvel, A. & Veel, P. (2016). *Jaarverslag beheer spanjaards duin 2016*. Zuid-Hollands Landschap.
- Arens, S., Beekman, W., Poot, S. & Veel, P. (2018). *Jaarverslag beheer spanjaards duin 2018*. Zuid-Hollands Landschap.
- Arens, S., Schaars, F., Beekman, W., Caljé, R., Vertegaal, K., van der Valk, M. & Paas, M. (2013). *Jaarverslag beheer spanjaards duin 2013*. Zuid-Hollands Landschap.
- Baas, A. & Nield, J. (2010). Ecogeomorphic state variables and phase-space construction for quantifying the evolution of vegetated aeolian landscapes. *Earth Surface Processes and Landforms*, 35(6), 717–731. doi:10.1002/esp.1990
- Bagnold, R. (1936). The movement of desert sand. *The Geographical Journal*, 157(892), 594–620. doi:10.1098/rspa.1936.0218
- Bagnold, R. (1937). The transport of sand by wind. *The Geographical Journal*, 89(5), 409–438. doi:10.2307/1786411
- Balke, T., Webb, E., van den Elzen, E., Galli, D., Herman, P. & Bouma, T. (2013). Seedling establishment in a dynamic sedimentary environment: A conceptual framework using mangroves. *Journal of Applied Ecology*, 50(3), 740–747. doi:10.1111/1365-2664.12067
- Baptist, M., Gerkema, T., van Prooijen, B., van Maren, D., van Regteren, M., Schulz, K., Colosimo, I., Vroom, J., van Kessel, T., Grasmeyer, B., Willemsen, P., Elschoot, K., de Groot, A., Cleveringa, J., van Eekelen, E., Schuurman, F., de Lange, H. & van Puijenbroek, M. (2019). Beneficial use of dredged sediment to enhance salt marsh development by applying a ‘mud motor’. *Ecological Engineering*, 127, 312–323. doi:10.1016/j.ecoleng.2018.11.019
- Bauer, B. & Davidson-Arnott, R. (2003). A general framework for modeling sediment supply to coastal dunes including wind angle, beach geometry, and fetch effects. *Geomorphology*, 49(1), 89–108. doi:10.1016/S0169-555X(02)00165-4
- Bauer, B., Davidson-Arnott, R., Hesp, P., Namikas, S., Ollerhead, J. & Walker, I. (2009). Aeolian sediment transport on a beach: Surface moisture, wind fetch, and mean transport. *Geomorphology*, 105(1), 106–116. doi:10.1016/j.geomorph.2008.02.016
- Bauer, B., Davidson-Arnott, R., Walker, I., Hesp, P. & Ollerhead, J. (2012). Wind direction and complex sediment transport response across a beach-dune system. *Earth Surface Processes and Landforms*, 37, 1661–1677. doi:10.1002/esp.3306
- Bernoulli, D. (1738). *Hydrodynamica, sive de viribus et motibus fluidorum commentarii : opus academicum ab auctore, dum Petropoli ageret, congestum*. doi:10.3931/e-rara-3911

- Best, J. (1993). On the interactions between turbulent flow structure, sediment transport and bed-form development: Some considerations from recent experimental research. *Unknown Journal*, 61–92.
- Cohn, N., Hoonhout, B., Goldstein, E., Vries, S., Moore, L., Durán, O. & Ruggiero, P. (2019). Exploring marine and aeolian controls on coastal foredune growth using a coupled numerical model. *Journal of Marine Science and Engineering*, 7, 13. doi:10.3390/jmse7010013
- de Graaf, H., Oude Elberink, S., Bollweg, A., Brügelmann, R. & Richardson, L. (2003). *Inwinning "droge" jarkus profielen langs nederlandse kust*.
- de Klerk, R. (2019). *The influence of buildings on aeolian coastal dune development* (Master's thesis, TU Delft).
- de Vriend, H., van Koningsveld, M. & Aarninkhof, S. (2014). 'building with nature': The new dutch approach to coastal and river works. *ICE Proceedings Civil Engineering*, 167, 18–24. doi:10.1680/cien.13.00003
- de Weger, R. (2017). *Rpas monitoring spanjaards duin - t2*. Shore Monitoring & Research.
- de Zeeuw, R. (2016). *Rpas monitoring spanjaards duin - t0*. Shore Monitoring & Research.
- Delgado-Fernandez, I. & Davidson-Arnott, R. (2011). Meso-scale aeolian sediment input to coastal dunes: The nature of aeolian transport events. *Geomorphology*, 126(1), 217–232. doi:10.1016/j.geomorph.2010.11.005
- Duarte Campos, L. (2018). *Quantification methods for aeolian sand transport on beaches* (Doctoral dissertation, University of Twente). doi:10.3990/1.9789036546676
- Eleveld, M. (1999). *Exploring coastal morphodynamics of ameland (the netherlands) with remote sensing monitoring techniques and dynamic modelling in gis* (Doctoral dissertation, Universiteit van Amsterdam).
- Eleveld, M. & van der Valk, B. (2019). *Memo: Stand van zaken rietpoot-experiment*. Deltares.
- Gulden, F. (2018). *Hoogtemeting spanjaardsduin - t4*. Shore Monitoring & Research.
- Hacker, S., Zarnetske, P., Seabloom, E., Ruggiero, P., Mull, J., Gerrity, S. & Jones, C. (2012). Subtle differences in two non-native congeneric beach grasses significantly affect their colonization, spread, and impact. *Oikos*, 121(1), 138–148. doi:10.1111/j.1600-0706.2011.18887.x
- Hesp, P. (2002). Foredunes and blowouts: Initiation, geomorphology and dynamics. *Geomorphology*, 48(1), 245–268. 29th Binghamton Geomorphology Symposium: Coastal Geomorphology. doi:10.1016/S0169-555X(02)00184-8
- Hillen, R. & de Ruij, J. (1993). *De basiskustlijn, norm voor dynamisch handhaven*. Rijkswaterstaat.
- Hoonhout, B. (2019). *Aeolis documentation, realease 1.0*.
- Hoonhout, B. & de Vries, S. (2016). A process-based model for aeolian sediment transport and spatiotemporal varying sediment availability. *Journal of Geophysical Research: Earth Surface*, 121(8), 1555–1575. doi:10.1002/2015JF003692
- Hoonhout, B. & de Vries, S. (2017). Aeolian sediment supply at a mega nourishment. *Coastal Engineering*, 123, 11–20. doi:10.1016/j.coastaleng.2017.03.001
- Houser, C. & Ellis, J. (2013). Beach and dune interaction. In *John F. Schroder (ed) Treatise on Geomorphology* (pp. 267–288). San Diego: Academic Press.
- Huiskes, A. (1979). *Ammophila arenaria* (L.) Link (psamma arenaria (L.) Roem. et Schult.; Calamagrostis arenaria (L.) Roth). *Journal of Ecology*, 67(1), 363–382. Retrieved from <http://www.jstor.org/stable/2259356>
- IJff, S., van der Valk, B. & van der Meulen, F. (2017). *Leidraad beheer spanjaards duin*. Deltares.

- Jackson, N. & Nordstrom, K. (2011). Aeolian sediment transport and landforms in managed coastal systems: A review. *Aeolian Research*, 3(2), 181–196. doi:10.1016/j.aeolia.2011.03.011
- Keijsers, J., de Groot, A. & Riksen, M. (2016). Modeling the biogeomorphic evolution of coastal dunes in response to climate change. *Journal of Geophysical Research: Earth Surface*, 121(6), 1161–1181. doi:10.1002/2015JF003815
- KNMI. (2020). Uurgegevens van het weer in nederland. <http://projects.knmi.nl/klimatologie/uurgegevens/selectie.cgi>.
- Kroy, K., Sauermann, G. & Herrmann, H. (2002). Minimal model for aeolian sand dunes. *Physical Review E*, 66, 31–302. doi:10.1103/PhysRevE.66.031302
- Maun, M. (1998). Adaptations of plants to burial in coastal sand dunes. *Canadian Journal of Botany*, 76(5), 713–738. doi:10.1139/b98-058
- Nickling, W. & McKenna Neuman, C. (2009). Aeolian sediment transport. (pp. 517–555). doi:10.1007/978-1-4020-5719-9_17
- Raupach, M. (1992). Drag and drag partition on rough surfaces. *Boundary-Layer Meteorology*, 60(4), 375–395. doi:10.1007/BF00155203
- Raupach, M., Gillette, D. & Leys, J. (1993). The effect of roughness elements on wind erosion threshold. *Journal of Geophysical Research: Atmospheres*, 98(D2), 3023–3029. doi:10.1029/92JD01922
- Reijers, V., Siteur, K., Hoeks, S., van Belzen, J., Borst, A., Heusinkveld, J., Govers, L., Bouma, T., Lamers, L., van de Koppel, J. & van der Heide, T. (2019). A lévy expansion strategy optimizes early dune building by beach grasses. *Nature Communications*, 10(1). doi:10.1038/s41467-019-10699-8
- Rijkswaterstaat. (2020). Rijkswaterstaat waterinfo. <https://waterinfo.rws.nl>.
- Roelvink, D. & Costas, S. (2019). Coupling nearshore and aeolian processes: Xbeach and duna process-based models. *Environmental Modelling & Software*, 115, 98–112. doi:10.1016/j.envsoft.2019.02.010
- Sauermann, G., Kroy, K. & Herrmann, H. (2001). Continuum saltation model for sand dunes. *Physical Review E*, 64, 031305. doi:10.1103/PhysRevE.64.031305
- Schaminée, J., Weeda, E. & Westhoff, V. (1998). *De vegetatie van nederland*. Opulus Press.
- Shelford, V. E. (1931). Some concepts of bioecology. *Ecology*, 12(3), 455–467. doi:10.2307/1928991
- Sherman, D. & Bauer, B. (1993). Dynamics of beach-dune systems. *Progress in Physical Geography: Earth and Environment*, 17(4), 413–447. doi:10.1177/030913339301700402
- Sherman, D. & Li, B. (2012). Predicting aeolian sand transport rates: A reevaluation of models. *Aeolian Research*, 3(4), 371–378. The 7th International Conference on Aeolian Research (ICAR VII), Santa Rosa, Argentina. doi:10.1016/j.aeolia.2011.06.002
- Van der Wal, D. (2000). Grain-size-selective aeolian sand transport on a nourished beach. *Journal of coastal research*, 16(3), 896–908.
- van der Meulen, F., van der Valk, B., Baars, L., Schoor, E. & van Woerden, H. (2014). Development of new dunes in the Dutch Delta: nature compensation and ‘building with nature’. *Journal of Coastal Conservation*, 18(5), 505–513. doi:10.1007/s11852-014-0315-2
- van Puijenbroek, M., Nolet, C., de Groot, A., Suomalainen, J., Riksen, M., Berendse, F. & Limpens, J. (2017). Exploring the contributions of vegetation and dune size to early dune development using unmanned aerial vehicle (uav) imaging. *Biogeosciences*, 14(23), 5533–5549. doi:10.5194/bg-14-5533-2017
- van Westen, B. (2018). *Numerical modelling of aeolian coastal landform development* (Master’s thesis, TU Delft).

- Verkerk, M. (2019). *Hoogtemeting spanjaardsduin - t5*. Shore Monitoring & Research.
- Vertegaal, C., Arens, S. & Reitsma, J. (2016). *Monitoring pilot zandmotor, onderdeel duinen*. Witteveen+Bos.
- Walker, I. & Nickling, W. (2002). Dynamic of secondary airflow and sediment transport over and in the lee of transverse dunes. *Progress in Physical Geography*, 26, 47–75. doi:10.1191/0309133302pp325ra
- Weng, W., Hunt, J., Carruthers, D., Warren, A., Wiggs, G., Livingstone, I. & Castro, I. (1991). Air flow and sand transport over sand-dunes. In O. Barndorff-Nielsen & B. Willetts (Eds.), *Aeolian grain transport* (pp. 1–22). Vienna: Springer Vienna.
- Wolfe, S. & Nickling, W. (1993). The protective role of sparse vegetation in wind erosion. *Progress in Physical Geography: Earth and Environment*, 17(1), 50–68. doi:10.1177/030913339301700104
- Ye, X., Yu, F. & Dong, M. (2006). A Trade-off Between Guerrilla and Phalanx Growth Forms in *Leymus secalinus* Under Different Nutrient Supplies. *Annals of Botany*, 98(1), 187–191. doi:10.1093/aob/mcl086
- Zarnetske, P., Hacker, S., Seabloom, E., Ruggiero, P., Killian, J., Maddux, T. & Cox, D. (2012). Biophysical feedback mediates effects of invasive grasses on coastal dune shape. *Ecology*, 93, 1439–50. doi:10.1890/11-1112.1